Linearized domain decomposition methods for two-phase porous media flow models involving dynamic capillarity and hysteresis

Available online at www.sciencedirect.com
ScienceDirect
Comput. Methods Appl. Mech. Engrg. 372 (2020) 113364
Computer methods in applied mechanics and engineering
www.elsevier.com/locate/cma

Linearized domain decomposition methods for two-phase porous media flow models involving dynamic capillarity and hysteresis

Stephan Benjamin Lunowa[a,*], Iuliu Sorin Pop[a,b], Barry Koren[c]

[a] UHasselt – Hasselt University, Computational Mathematics, Agoralaan, 3590 Diepenbeek, Belgium
[b] University of Bergen, Department of Mathematics, P.O. Box 7803, 5020 Bergen, Norway
[c] Eindhoven University of Technology, Department of Mathematics and Computer Science, P.O. Box 513, 5600MB Eindhoven, The Netherlands

Received 18 March 2020; received in revised form 29 June 2020; accepted 3 August 2020
Available online 3 September 2020

Abstract

We discuss two linearization and domain decomposition methods for mathematical models for two-phase flow in a porous medium. The medium consists of two adjacent regions with possibly different parameterizations. The model accounts for non-equilibrium effects like dynamic capillarity and hysteresis. The θ-scheme is adopted for the temporal discretization of the equations yielding nonlinear time-discrete equations. For these, we propose and analyze two iterative schemes, which combine a stabilized linearization iteration of fixed-point type, the L-scheme, and a non-overlapping domain decomposition method into one iteration. First, we prove the existence of unique solutions to the problems defining the linear iterations. Then, we give the rigorous convergence proof for both iterative schemes towards the solution of the time-discrete equations.

The developed schemes are independent of the spatial discretization or the mesh and avoid the use of derivatives as in Newton based iterations. Their convergence holds independently of the initial guess, and under mild constraints on the time step. The numerical examples confirm the theoretical results and demonstrate the robustness of the schemes. In particular, the second scheme is well suited for models incorporating hysteresis. The schemes can be easily implemented for realistic applications.

MSC: 65M55; 35K55; 76S05

Keywords: Linearization; Domain decomposition; Two-phase flow in porous media; Dynamic capillarity; Hysteresis

1. Introduction

Porous media flow has been a research field of ongoing interest for years with prominent applications such as CO_2 storage, groundwater pollution and enhanced oil recovery. Understanding the underlying phenomena is crucial for the prediction of these subsurface processes. But measurements are very expensive, if feasible at all, so that mathematical modeling and simulation are the most important tools to gain further insight. The mathematical models typically consist of coupled nonlinear differential equations, which may degenerate and change type in an a-priori unknown manner, depending on the solution itself. While the complexity increases further when dynamic

* Corresponding author.
E-mail addresses: stephan.lunowa@uhasselt.be (S.B. Lunowa), sorin.pop@uhasselt.be (I.S. Pop), b.koren@tue.nl (B. Koren).

https://doi.org/10.1016/j.cma.2020.113364
0045-7825/

and hysteretic effects are incorporated, largely varying or even discontinuous physical properties pose additional difficulties. There is a strong demand for the mathematical design and analysis of suitable, robust computational methods.

Newton based solvers cannot be applied directly to these problems due to severe constraints on the time step sizes to ensure convergence [1]. A simple fixed-point type iteration, the L-scheme, has been proposed as alternative. The high robustness of this method comes at the price of a slower, only linear convergence. The solution method is independent of the spatial discretization. It is combined with the (mixed) finite element method in [2,3] for Richards' equation, with equilibrium capillary pressure and two-phase flow with dynamic capillarity, respectively. The approach is used in [4] as a preconditioner for the Newton method. In [5], the L-scheme is used together with a discontinuous Galerkin method for the two-phase system with dynamic effects, neglecting hysteresis. A multi-point flux approximation finite volume method is applied in [6] for two-phase flow incorporating dynamic capillarity. Whereas the analysis is commonly accomplished assuming Lipschitz continuous parameter functions, it is extended in [7,8] to Richards' and two-phase equations, involving only Hölder continuous coefficients, such as the often used van-Genuchten–Mualem parameterization.

In the situation of layered soil, it seems natural to additionally apply a domain decomposition method to decouple the essentially different layers and thereby speeding up the convergence. Though stemming from 1870 [9], domain decomposition methods became subject to intensive research only 100 years later, starting with [10,11]. Henceforth, it became used and optimized for a wide range of applications, see e.g. [12–16]. In [17], a non-overlapping domain decomposition method is analyzed for nonlinear convection-diffusion equations in a time-continuous setting. Such methods can also be used after temporal discretization for porous media equations, as proposed in [18,19] for a simplistic setting, while Richards' equation and the two-phase flow equations are considered in [20,21], where a-posteriori error estimates and multirate time stepping methods are derived. In [22,23], the domain decomposition is integrated in the linearization process for both Richards' equation and two-phase flow, and the convergence is proven rigorously. For single-phase flow in a fractured medium, a domain decomposition method is used together with the L-scheme in [24] to solve the mixed-dimensional problem.

Here, we propose two linearization and domain decomposition schemes for two-phase flow in block-heterogeneous porous media. The model includes dynamic effects and hysteresis in the capillary pressure formulation. These methods are independent of the concrete space discretization and avoid the use of derivatives as in Newton based iterations. By maintaining the formulation of the equations in physical variables like saturation and pressure, instead of using the Kirchhoff transformation, these schemes are particularly accessible for direct application in the engineering context. This work generalizes and substantiates the preliminary results reported in [25,26].

This article is structured in the following way: The two-phase flow model, the notation and the assumptions are introduced in Section 2. In Section 3, the temporal discretization by the θ-scheme is stated. Based on this, the iterative schemes for finding the solutions to the nonlinear semi-discrete equations are derived. The analysis in Section 4 contains proofs for the existence of unique solutions to the problems defining the linear iterations and for the convergence of the iterative solutions. Section 5 addresses the numerical validation of the theoretical results by several examples in two spatial dimensions. Finally, Section 6 completes this work with a discussion and outlook.

2. Mathematical model of non-equilibrium two-phase flow in porous media

Let the domain $\Omega \subset \mathbb{R}^d$ for $d \in \mathbb{N}$ with a Lipschitz boundary $\partial\Omega$ and the final time $T > 0$ be fixed. The domain is partitioned into two disjoint subdomains Ω_1 and Ω_2 with Lipschitz boundaries $\partial\Omega_l$ and outer normal vectors $\boldsymbol{\nu}_l$ for $l \in \{1, 2\}$, which henceforth denotes the subdomain index. Furthermore, the subdomains are separated by the interface $\Gamma = \Omega \setminus (\Omega_1 \cup \Omega_2)$, which is assumed to be a $(d-1)$-dimensional manifold (see also Fig. 1). Note that the extension of this and all the following to more than two subdomains is straightforward, see [22, Remark 3 & Section 4.4]. All the following quantities can depend on their position in the domain, but we suppress this dependence for the ease of presentation. In each subdomain Ω_l, the dimensionless formulation for flow of two immiscible, incompressible phases through a stationary, rigid porous medium is governed by the mass balance equations

$$-\phi_l \partial_t s_l + \nabla\cdot \boldsymbol{u}_{n,l} = q_{n,l} \quad \text{in } \Omega_l \times (0,T), \tag{2.1}$$

$$\phi_l \partial_t s_l + \nabla\cdot \boldsymbol{u}_{w,l} = q_{w,l} \quad \text{in } \Omega_l \times (0,T), \tag{2.2}$$

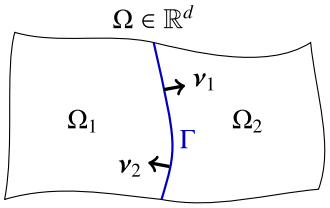

Fig. 1. Schematic sketch of a block-heterogeneous domain $\Omega = \Omega_1 \cup \Gamma \cup \Omega_2$ with interface Γ.

where $\phi_l \in (0, 1)$ is the medium porosity and s_l is the saturation of the wetting phase (note that in a two-phase system $s_n + s_w = 1$, i.e. only one saturation is necessary). The source rate of the α-phase ($\alpha \in \{n, w\}$) is denoted by $q_{\alpha,l}$. The specific discharge $\boldsymbol{u}_{\alpha,l}$ of the α-phase incorporates the intrinsic permeability K_l, which is a second rank tensor for anisotropic media, and the relative mobility $\lambda_{\alpha,l}$ due to the extended Darcy law,

$$\boldsymbol{u}_{\alpha,l} = -\lambda_{\alpha,l}(s_l) K_l \nabla p_{\alpha,l} \quad \text{in } \Omega_l \times (0, T). \tag{2.3}$$

Here, $p_{\alpha,l}$ denotes the pressure in the α-phase. Note that addition of (2.1) and (2.2) implies that the total discharge $\boldsymbol{u}_{n,l} + \boldsymbol{u}_{w,l}$ is divergence free whenever the total source rate $q_{n,l} + q_{w,l}$ vanishes.

At the interface Γ separating the two subdomains, we assume that the normal flux and the pressure of each phase are continuous, i.e. for $\alpha \in \{n, w\}$

$$\boldsymbol{u}_{\alpha,1} \cdot \boldsymbol{\nu}_1 = -\boldsymbol{u}_{\alpha,2} \cdot \boldsymbol{\nu}_2, \quad p_{\alpha,1} = p_{\alpha,2} \quad \text{on } \Gamma \times (0, T). \tag{2.4}$$

Remark 2.1 (*Interface Conditions*)**.** The continuity of the normal fluxes follows directly from mass conservation. The continuity of the phase pressure is valid, if the phase is present at both sides of the interface. This is not necessarily valid any more for so-called entry-pressure models, when the non-wetting phase is absent at one side of the interface, as shown in [27–29] for standard models and in [30] for dynamic capillary pressure. To the best of our knowledge, conditions for entry-pressure models including both dynamic and hysteretic effects have not yet been proposed or derived.

Typically, one assumes that the phase-pressure difference $p_n - p_w$ is a function of the wetting saturation, the so-called equilibrium capillary pressure $p_c(s_w)$, which can be obtained by experiments under quasi-equilibrium conditions. But the experimental results reported e.g. in [31–34] are ruled out by this standard model. To deal with this, non-equilibrium models incorporating dynamic effects and hysteresis are studied in e.g. [35–41]. Here, we consider the play-type hysteresis model proposed in [42,43],

$$p_{n,l} - p_{w,l} \in p_{c,l}(s_l) - \gamma_l \operatorname{sign}(\partial_t s_l) - \tau_l(s_l)\partial_t s_l, \tag{2.5}$$

where $\gamma_l \geq 0$ and the non-negative function τ_l are used to model the effects due to hysteresis and dynamic capillarity, respectively. We refer to [44–47] for a mathematical investigation of saturation overshoots or finger-type profiles.

Below, we will also use a regularization $\Phi_{\delta,l}$ of the scaled sign function to obtain a single-valued relation and to ensure strict monotonicity. For fixed, small parameter $\delta > 0$ and $l \in \{1, 2\}$, the regularization is given by

$$\Phi_{\delta,l}(\xi) = \begin{cases} \gamma_l \operatorname{sign}(\xi) & \text{if } |\xi| \geq \delta, \\ \gamma_l \frac{\xi}{\delta} & \text{if } |\xi| < \delta. \end{cases}$$

The regularized non-equilibrium capillary pressure condition then becomes

$$p_{n,l} - p_{w,l} = p_{c,l}(s_l) - \Phi_{\delta,l}(\partial_t s_l) - \partial_t T_l(s_l) \quad \text{in } \Omega_l \times (0, T), \tag{2.6}$$

where T_l denotes the primitive of τ_l.

For uniformly positive τ, the multi-valued Eq. (2.5) can be solved in $\partial_t s$, as done in [48–50]. This yields a single-valued function $\hat{\Psi}_l$, such that one can rewrite the capillary pressure relation in the inverted form $\partial_t s_l = \hat{\Psi}_l(s_l, p_{n,l} - p_{w,l})$. This formulation has the major advantage that it imposes explicit values for the time derivative of the saturation, and avoids a multi-valued relation like (2.5). Here, we consider the inverse capillary pressure condition only for constant $\tau_l > 0$, which then becomes

$$\partial_t s_l = \Psi_l(p_{n,l} - p_{w,l} - p_{c,l}(s_l)) \quad \text{in } \Omega_l \times (0, T), \tag{2.7}$$

where

$$\Psi_l(p) = \begin{cases} \frac{-p+\gamma_l}{\tau_l} & \text{if } p \geq \gamma_l, \\ 0 & \text{if } |p| < \gamma_l, \\ \frac{-p-\gamma_l}{\tau_l} & \text{if } p \leq -\gamma_l. \end{cases}$$

A regularization of Ψ_l matching $\Phi_{\delta,l}$ is used in [44,46,49,51] to prove the existence of weak solutions for $\delta \to 0$, and to develop appropriate numerical schemes. Moreover, it is possible to only include hysteresis and no dynamic effects. Then, Ψ_l has to be regularized by including e.g. a small dynamic effect, namely taking $\tau_l = \varepsilon > 0$.

Remark 2.2. Richards' equation models unsaturated flow in porous media [52], based on the simplification that the non-wetting pressure p_n is constant, such that (2.1) can be neglected. Although this paper focuses on the general two-phase flow equations, the results can be directly transferred to Richards' equation.

2.1. Notation

We denote by $L^2(X)$, $H^1(X)$, $H^1_0(X)$ and $H^{\text{div}}(X)$ the standard Hilbert spaces on $X \in \{\Omega, \Omega_1, \Omega_2\}$. $H^{1/2}(\Gamma)$ consists of all traces of functions in $H^1(\Omega)$. This trace on Γ of $w \in H^1(\Omega)$ is denoted by $w|_\Gamma$. For any function $f \in L^2(\Omega)$, $f_l := f|_{\Omega_l}$ denotes the restriction to Ω_l for $l \in \{1, 2\}$. Vice versa, a pair of functions $(f_1, f_2) \in L^2(\Omega_1) \times L^2(\Omega_2)$ is identified with the natural L^2-extension f on the whole domain Ω. For simplicity, we only consider homogeneous Dirichlet boundary conditions at $\partial\Omega$ for the pressures, so that the following spaces will be used

$$\mathcal{W}_l := \left\{ w \in H^1(\Omega_l) \,:\, w|_{\partial\Omega_l \cap \partial\Omega} \equiv 0 \right\}, \qquad \mathcal{W} := L^2(\Omega) \times [\mathcal{W}_1 \times \mathcal{W}_2]^2.$$

At the expense of additional technical effort, it is possible to extend the results in this article to other types of boundary conditions. Since $\partial\Omega \cap \partial\Omega_l$ is either empty or has positive $(d-1)$-measure, the functions in $\mathcal{W}_l$ vanish on this common part of the boundary. Note that $w \in H^1_0(\Omega)$ is equivalent to $(w_1, w_2) \in \mathcal{W}_1 \times \mathcal{W}_2$ with $w_1|_\Gamma \equiv w_2|_\Gamma$. This is a direct consequence of the trace theorem. For the continuity of the pressure across the interface Γ, we introduce the space

$$\mathcal{V} := L^2(\Omega) \times [H^1_0(\Omega)]^2.$$

Moreover, the space for the interface conditions on Γ is given by

$$H^{1/2}_{00}(\Gamma) := \left\{ w \in H^{1/2}(\Gamma) \,:\, \exists v \in H^1_0(\Omega) \,:\, v|_\Gamma \equiv w \right\}.$$

It is a Hilbert space as the quotient space $H^1_0(\Omega)/\ker(\cdot|_\Gamma)$, see [53, Proposition 2.3]. The L^2 inner product and norm on $X \in \{\Omega_1, \Omega_2, \Gamma\}$ are denoted by $(\cdot,\cdot)_X$ and $\|\cdot\|_X$. Analogously, $\langle\cdot,\cdot\rangle_\Gamma$ stands for the dual pairing on $H^{1/2}_{00}(\Gamma)$ with $H^{1/2}_{00}(\Gamma)'$ via the Gelfand triple with $L^2(\Gamma)$. Here and in the following, the dual of a Banach space B is denoted by B'.

2.2. Assumptions on the coefficient functions

In the following, we summarize all assumptions on the coefficient functions, which are mostly also found in realistic physical systems. Note that we explicitly exclude the degeneration of the equations by requiring positive mobilities λ_α and a Lipschitz continuous equilibrium capillary pressure p_c. This is necessary to ensure that the pressures p_w, p_n based on (2.1)–(2.3) are well-defined even if one phase is not present due to $s = 0, 1$. In realistic applications, where these assumptions do not hold, one can use a regularization like in [50,54–57], where the convergence of the solutions of the regularized equations towards the solution of the degenerated equations and the existence of the latter solutions are proven. Note that we allow discontinuities of the coefficient functions at the interface Γ.

Assumption 1. For $l \in \{1, 2\}$ and $\alpha \in \{n, w\}$, assume that

- $K_l : \Omega_l \to \mathbb{R}^{d\times d}$ is symmetric, and constants $\underline{K}_l, \overline{K}_l \in \mathbb{R}^+ = (0, \infty)$ exist such that $\underline{K}_l \|\xi\|^2_{\mathbb{R}^d} \leq \xi^T K_l(x)\xi \leq \overline{K}_l \|\xi\|^2_{\mathbb{R}^d}$ for all $x \in \Omega_l$ and $\xi \in \mathbb{R}^d$,

- $\lambda_{\alpha,l} : \mathbb{R} \to \mathbb{R}^+$, is Lipschitz continuous with Lipschitz constant $L_{\lambda_\alpha,l}$, and constants $m_{\lambda_\alpha,l}, M_{\lambda_\alpha,l} \in \mathbb{R}^+$ exist such that $m_{\lambda_\alpha,l} \leq \lambda_{\alpha,l}(s) \leq M_{\lambda_\alpha,l}$ for all $s \in \mathbb{R}$,
- $q_{\alpha,l} : [0, T] \to L^2(\Omega_l)$ is continuous,
- $p_{c,l} : \mathbb{R} \times \Omega_l \to \mathbb{R}$ is strictly monotonically decreasing in the first variable, Lipschitz continuous, and constants $m_{p_c,l}, L_{p_c,l} \in \mathbb{R}^+$ exist such that $m_{p_c,l} |r - s| \leq \left| p_{c,l}(r, x) - p_{c,l}(s, x) \right| \leq L_{p_c,l} |r - s|$ for all $r, s \in \mathbb{R}$ and $x \in \Omega_l$,
- $\tau_l : \mathbb{R} \to \mathbb{R}^+$ is measurable, and constants $m_{T,l}, L_{T,l} \in \mathbb{R}^+$ exist such that $m_{T,l} < \tau_l(s) < L_{T,l}$ for all $s \in \mathbb{R}$; we call its primitive $T_l : \mathbb{R} \to \mathbb{R}$,
- $\gamma_l : \Omega_l \to [0, \infty)$ is Lipschitz continuous and bounded by a constant $M_{\gamma,l} \in \mathbb{R}^+$.

Remark 2.3. The extension of $\lambda_{\alpha,l}$, $p_{c,l}$ and τ_l to any value $s \in \mathbb{R}$ is necessary because the non-degenerated, non-equilibrium model does not satisfy a maximum principle due to possible overshoots. The solutions of the degenerated model remain (essentially) bounded, see [55,56]. These extensions can be constructed naturally, only assuming Lipschitz continuity on [0, 1].

Remark 2.4. By Assumption 1, $\Phi_{\delta,l} : \mathbb{R} \times \Omega_l \to \mathbb{R}$ is monotonically increasing in the first variable and Lipschitz continuous with Lipschitz constant $L_{\Phi_\delta,l} = M_{\gamma,l}/\delta$. Furthermore for constant $\tau_l > 0$, $\Psi_l : \mathbb{R} \times \Omega_l \to \mathbb{R}$ is Lipschitz continuous, monotonically decreasing in the first variable, and it holds $|\Psi_l(p, x) - \Psi_l(q, x)| \leq L_{\Psi,l} |p - q|$ for all $p, q \in \mathbb{R}$ and $x \in \Omega_l$, where $L_{\Psi,l} = \tau_l^{-1}$.

The system of nonlinear equations (2.1)–(2.4) with either (2.6) or (2.7) forms an initial–boundary-value problem in the primary variables s, p_n and p_w for given initial data $s|_{t=0} = s^0 \in L^\infty(\Omega; [0, 1])$.

Remark 2.5 (*Existence and Boundedness of Unique Weak Solutions*)**.** For the existence of unique weak solutions to (2.1)–(2.4) under either condition (2.6) or (2.7), with respect to initial and boundary conditions, we refer to [49,50,58]. The existence of solutions is proven in [49], while the uniqueness of the solutions to these equations for $\delta = 0$ is derived in [50,58]. Note that additional assumptions on the regularity of the coefficient functions and the domain are necessary for this. Furthermore, the sequence of solutions to the regularized equations converge (weakly) towards the solution of the original equations for $\delta \to 0$, as shown in [51].

For the main theorems Theorems 4.1 and 4.2 in this work we assume the existence of time-discrete solutions with bounded pressure gradients. This has been proven in the time-continuous case e.g. in [50, Lemma 1], where $s \in L^\infty(0, T; C^{0,\beta}(\overline{\Omega}))$ and $p_n, p_w \in L^\infty(0, T; C^{1,\beta}(\overline{\Omega}))$ is obtained under the above mentioned additional regularity assumptions that the coefficient functions are independent of $\boldsymbol{x}$, that $p_c \in C^1$ and $s^0 \in C^{0,\beta}(\Omega)$, and that Ω is a $C^{1,\beta}$-domain.

3. Temporal discretization and iterative schemes

First, we present the discretization in time by the θ-scheme. In particular, we are interested in the unconditionally stable situation when $\theta \geq 1/2$. For $\theta = 1$, this boils down to the first-order backward Euler method, while $\theta = 1/2$ coincides with the second-order Crank–Nicolson method. The resulting semi-discrete equations are nonlinear, and thus iterative methods are necessary to find the solutions. We propose two linearization and domain decomposition schemes (LDD-schemes).

3.1. Discretization in time

For given $N \in \mathbb{N}$, let the fixed time step length be $\Delta t := \frac{T}{N}$. At time $t^k := k\Delta t$, the approximations of the saturation, pressures and source terms are denoted by s^k, p_α^k, q_α^k. With this, the auxiliary quantities at time t^k are

$$\boldsymbol{u}_{\alpha,l}^k := -\lambda_{\alpha,l}(s_l^k) K_l \nabla p_{\alpha,l}^k, \qquad p_{c,l}^k := p_{c,l}(s_l^k), \qquad \Psi_l^k := \Psi_l(p_{n,l}^k - p_{w,l}^k - p_{c,l}^k).$$

For $\theta \in (0, 1]$, the θ-averaged quantities are defined by $(\cdot)^{k,\theta} := \theta(\cdot)^k + (1-\theta)(\cdot)^{k-1}$, e.g. $\boldsymbol{u}_{\alpha,l}^{k,\theta} = \theta \boldsymbol{u}_{\alpha,l}^k + (1-\theta)\boldsymbol{u}_{\alpha,l}^{k-1}$. Then, the interface conditions (2.4) directly become

$$\boldsymbol{u}_{\alpha,1}^{k,\theta} \cdot \boldsymbol{\nu}_1 = -\boldsymbol{u}_{\alpha,2}^{k,\theta} \cdot \boldsymbol{\nu}_2, \quad p_{\alpha,1}^k = p_{\alpha,2}^k \quad \text{on } \Gamma. \tag{3.1}$$

The time-discrete counterparts of (2.1) and (2.2) are tested with $\xi_n, \xi_w \in H_0^1(\Omega)$. After partial integration using (3.1) and summation over $l \in \{1, 2\}$, the time-discrete, weak equations read

$$\sum_{l=1}^{2}\left(-\phi_l \left(\tfrac{s_l^k - s_l^{k-1}}{\Delta t},\ \xi_{n,l}\right)_{\Omega_l} - \left(\boldsymbol{u}_{n,l}^{k,\theta},\ \nabla \xi_{n,l}\right)_{\Omega_l}\right) = \left(q_{n,l}^{k,\theta},\ \xi_n\right)_{\Omega}, \tag{3.2}$$

$$\sum_{l=1}^{2}\left(\phi_l \left(\tfrac{s_l^k - s_l^{k-1}}{\Delta t},\ \xi_{w,l}\right)_{\Omega_l} - \left(\boldsymbol{u}_{w,l}^{k,\theta},\ \nabla \xi_{w,l}\right)_{\Omega_l}\right) = \left(q_{w,l}^{k,\theta},\ \xi_w\right)_{\Omega}. \tag{3.3}$$

Additionally, the time-discrete counterparts of either the regularized non-equilibrium capillary pressure equation (2.6)

$$p_{n,l}^{k,\theta} - p_{w,l}^{k,\theta} = p_{c,l}^{k,\theta} - \Phi_{\delta,l}\left(\tfrac{s_l^k - s_l^{k-1}}{\Delta t}\right) - \tfrac{T_l(s_l^k) - T_l(s_l^{k-1})}{\Delta t} \quad \text{in } L^2(\Omega_l) \text{ for } l \in \{1, 2\}, \tag{3.4}$$

or of the inverse capillary pressure equation (2.7)

$$\tfrac{s_l^k - s_l^{k-1}}{\Delta t} = \theta\, \Psi_l^k + (1-\theta)\, \Psi_l^{k-1} \quad \text{in } L^2(\Omega_l) \text{ for } l \in \{1, 2\}, \tag{3.5}$$

will be used below, yielding the following two semi-discrete formulations.

Problem 1 (*Semi-discrete Weak Formulation I*)**.** Given $(s^{k-1}, p_n^{k-1}, p_w^{k-1}) \in \mathcal{V}$, find $(s^k, p_n^k, p_w^k) \in \mathcal{V}$ such that (3.2)–(3.4) hold for all $\xi_n, \xi_w \in H_0^1(\Omega)$.

Problem 2 (*Semi-discrete Weak Formulation II*)**.** Given $(s^{k-1}, p_n^{k-1}, p_w^{k-1}) \in \mathcal{V}$, find $(s^k, p_n^k, p_w^k) \in \mathcal{V}$ such that (3.2), (3.3) and (3.5) hold for all $\xi_n, \xi_w \in H_0^1(\Omega)$.

In particular, the second formulation is well suited for hysteretic models since it avoids the regularization of the sign function, and thus additional errors. In the absence of hysteresis, the first formulation is more natural and can be straightforwardly used even for vanishing τ. Note that both weak semi-discrete problems are well defined.

Remark 3.1. If $(s^k, p_n^k, p_w^k) \in \mathcal{V}$ is a solution of Problem 1 or Problem 2, $p_{\alpha,1}^k|_\Gamma = p_{\alpha,2}^k|_\Gamma$ holds by the definition of $\mathcal{V}$. Since $s_l^k, s_l^{k-1}, q_\alpha^{k,\theta} \in L^2(\Omega_l)$, testing (3.2) and (3.3) with arbitrary $\xi_{\alpha,l} \in C_0^\infty(\Omega_l)$ implies $\nabla \cdot \boldsymbol{u}_{\alpha,l}^{k,\theta} \in L^2(\Omega_l)$, i.e. $\boldsymbol{u}_{\alpha,l}^{k,\theta} \in H^{\mathrm{div}}(\Omega_l)$. This shows that

$$\nabla \cdot \boldsymbol{u}_{n,l}^{k,\theta} = \phi_l \tfrac{s_l^k - s_l^{k-1}}{\Delta t} + q_{n,l}^{k,\theta}, \quad \nabla \cdot \boldsymbol{u}_{w,l}^{k,\theta} = -\phi_l \tfrac{s_l^k - s_l^{k-1}}{\Delta t} + q_{w,l}^{k,\theta} \quad \text{in } L^2(\Omega_l). \tag{3.6}$$

Therefore, the normal trace lemma [59, Lemma III.1.1] yields $\boldsymbol{u}_{\alpha,l}^{k,\theta} \cdot \boldsymbol{\nu}_l \in H^{1/2}(\partial\Omega_l)'$ and integration by parts in (3.2) and (3.3) implies $\boldsymbol{u}_{\alpha,1}^{k,\theta} \cdot \boldsymbol{\nu}_1 = -\boldsymbol{u}_{\alpha,2}^{k,\theta} \cdot \boldsymbol{\nu}_2$ in $H_{00}^{1/2}(\Gamma)'$.

Problems 1 and 2 are nonlinear systems of mixed elliptic algebraic equations with possibly discontinuous coefficients. This is evident when (3.5) is substituted into (3.2) and (3.3). One may prove the existence of (unique) solutions analogously to the time-continuous case (Remark 2.5) or the fully discrete case in [60] for equilibrium capillary pressure. By this, the time-discrete pressure gradients should be bounded — corresponding to the results in [50,60]. However, this lies out of the scope of this article. In the following, we will assume that solutions to Problems 1 and 2 with bounded gradients exist.

3.2. Linearization and domain decomposition schemes

To decouple the problems on the subdomains, and thereby to account for the possible discontinuities at the interface Γ, we introduce a non-overlapping domain decomposition method. Following the ideas in [11,61], we combine the interface conditions (3.1) by a (to be freely chosen) parameter $\mathcal{L}_\Gamma \in (0, \infty)$ to define

$$g_{\alpha,l}^k := \boldsymbol{u}_{\alpha,l}^{k,\theta} \cdot \boldsymbol{\nu}_l - \mathcal{L}_\Gamma\, p_{\alpha,l}^k$$

for $l \in \{1, 2\}$. With these Robin type expressions, the interface conditions (3.1) at Γ read

$$g_{\alpha,3-l}^k = -2\mathcal{L}_\Gamma\, p_{\alpha,l}^k - g_{\alpha,l}^k. \tag{3.7}$$

This formulation is equivalent to (3.1) for any $\mathcal{L}_\Gamma \neq 0$, cf. [22, Remark 1].

Lemma 3.1. *Let $k \in \mathbb{N}$ be fixed and assume that $(s^k, p_n^k, p_w^k) \in \mathcal{W}$ and $g_{\alpha,l}^k \in H_{00}^{1/2}(\Gamma)'$ exist for $l \in \{1,2\}$ and $\alpha \in \{n, w\}$, such that it holds*

$$-\phi_l \left(\tfrac{s_l^k - s_l^{k-1}}{\Delta t},\ \xi_{n,l} \right)_{\Omega_l} - \left(\boldsymbol{u}_{n,l}^{k,\theta},\ \nabla \xi_{n,l} \right)_{\Omega_l} + \left\langle \mathcal{L}_\Gamma p_{n,l}^k + g_{n,l}^k,\ \xi_{n,l} \right\rangle_\Gamma = \left(q_{n,l}^{k,\theta},\ \xi_{n,l} \right)_{\Omega_l}, \tag{3.8}$$

$$\phi_l \left(\tfrac{s_l^k - s_l^{k-1}}{\Delta t},\ \xi_{w,l} \right)_{\Omega_l} - \left(\boldsymbol{u}_{w,l}^{k,\theta},\ \nabla \xi_{w,l} \right)_{\Omega_l} + \left\langle \mathcal{L}_\Gamma p_{w,l}^k + g_{w,l}^k,\ \xi_{w,l} \right\rangle_\Gamma = \left(q_{w,l}^{k,\theta},\ \xi_{w,l} \right)_{\Omega_l}, \tag{3.9}$$

$$\left\langle g_{\alpha,l}^k,\ \xi_{\alpha,l} \right\rangle_\Gamma = \left\langle -2\mathcal{L}_\Gamma p_{\alpha,3-l}^k - g_{\alpha,3-l},\ \xi_{\alpha,l} \right\rangle_\Gamma, \tag{3.10}$$

for $l \in \{1,2\}$ and all $\xi_n, \xi_w \in H_0^1(\Omega)$, as well as either (3.4) or (3.5). Then, the interface conditions $\boldsymbol{u}_{\alpha,1}^{k,\theta} \cdot \boldsymbol{\nu}_1 = -\boldsymbol{u}_{\alpha,2}^{k,\theta} \cdot \boldsymbol{\nu}_2$ in $H_{00}^{1/2}(\Gamma)'$ and $p_{\alpha,1}^k|_\Gamma = p_{\alpha,2}^k|_\Gamma$ are satisfied, and thus $(s^k, p_n^k, p_w^k) \in \mathcal{V}$ is a solution of Problem 1 or Problem 2, respectively. Moreover, it holds $g_{\alpha,l}^k = \boldsymbol{u}_{\alpha,l}^{k,\theta} \cdot \boldsymbol{\nu}_l - \mathcal{L}_\Gamma p_{\alpha,l}^k$ in $H_{00}^{1/2}(\Gamma)'$.

Vice versa, if $(s^k, p_n^k, p_w^k) \in \mathcal{V}$ is a solution of Problem 1 or Problem 2, and we define

$$g_{\alpha,l}^k := \boldsymbol{u}_{\alpha,l}^{k,\theta} \cdot \boldsymbol{\nu}_l - \mathcal{L}_\Gamma p_{\alpha,l}^k \quad \text{in} \quad H_{00}^{1/2}(\Gamma)', \tag{3.11}$$

then (s^k, p_n^k, p_w^k) and $g_{\alpha,l}^k$, $l \in \{1,2\}$ and $\alpha \in \{n, w\}$, solve the system (3.8)–(3.10).

Proof. Subtracting Eqs. (3.10) for $l \in \{1,2\}$ directly yields $p_{\alpha,1}^k|_\Gamma = p_{\alpha,2}^k|_\Gamma$, whereas adding up these equations leads to $g_{\alpha,1}^k + g_{\alpha,2}^k = -\mathcal{L}_\Gamma(p_{\alpha,1}^k + p_{\alpha,2}^k)$. Using this in the sum of (3.8) over $l \in \{1,2\}$ gives (3.2). Analogously, one obtains (3.3) from (3.9). Together with (3.4) or (3.5), this is equivalent to Problem 1 or Problem 2, respectively. Furthermore, integration by parts in (3.8) and (3.9), using (3.6), leads to $g_{\alpha,l}^k = \boldsymbol{u}_{\alpha,l}^{k,\theta} \cdot \boldsymbol{\nu}_l - \mathcal{L}_\Gamma p_{\alpha,l}^k$ in $H_{00}^{1/2}(\Gamma)'$.

Conversely, if (s^k, p_n^k, p_w^k) solves Problem 1 or Problem 2, then the continuity of pressures and normal fluxes at Γ holds, and thus one gets

$$g_{\alpha,l}^k = \boldsymbol{u}_{\alpha,l}^{k,\theta} \cdot \boldsymbol{\nu}_l - \mathcal{L}_\Gamma p_{\alpha,l}^k = -\boldsymbol{u}_{\alpha,3-l}^{k,\theta} \cdot \boldsymbol{\nu}_{3-l} - \mathcal{L}_\Gamma p_{\alpha,3-l}^k = -2\mathcal{L}_\Gamma p_{\alpha,3-l}^k - g_{\alpha,3-l}^k \quad \text{in } H_{00}^{1/2}(\Gamma)'.$$

Finally, (3.8) and (3.9) follow from integration by parts of (3.2) and (3.3) using (3.6) and the definition of $g_{\alpha,l}^k$. □

The above-shown equivalence of Lemma 3.1 can also be observed for Richards' equation [22]. We will use the system (3.8)–(3.10) and either (3.4) or (3.5) instead of the equivalent semi-discrete Problems 1 and 2 to prove that the solutions to the LDD-schemes converge towards the solutions of Problems 1 and 2, respectively.

The two problems only differ in the used capillary pressure relation, but this will result in different iterative schemes, as will be seen below. The common idea is to linearize the capillary pressure equations (3.4) and (3.5), and to add stabilization terms of the form

$$\mathcal{L}(\text{solution of current iteration} - \text{solution of last iteration}),$$

which vanish in the limit if the sequence converges.

Assuming that for some $i \in \mathbb{N}$ the approximations $(s^{k,i-1}, p_n^{k,i-1}, p_w^{k,i-1}) \in \mathcal{W}$ and $g_{\alpha,l}^{k,i-1} \in L^2(\Gamma)$ for $l \in \{1,2\}$ and $\alpha \in \{n, w\}$ are known, the linearized fluxes and interface conditions are defined by

$$\boldsymbol{u}_{\alpha,l}^{k,\theta,i} := -\theta \lambda_{\alpha,l}(s_l^{k,j}) K_l \nabla p_{\alpha,l}^{k,i} + (1-\theta)\boldsymbol{u}_{\alpha,l}^{k-1}, \qquad g_{\alpha,l}^{k,i} := -2\mathcal{L}_\Gamma p_{\alpha,3-l}^{k,i-1} - g_{\alpha,3-l}^{k,i-1},$$

where $j = i-1$ for the following LDD-scheme I, while $j = i$ for the LDD-scheme II. With these, (3.2) and (3.3) become linear and decouple into

$$-\phi_l \left(\tfrac{s_l^{k,i} - s_l^{k-1}}{\Delta t},\ \xi_{n,l} \right)_{\Omega_l} - \left(\boldsymbol{u}_{n,l}^{k,\theta,i},\ \nabla \xi_{n,l} \right)_{\Omega_l} + \left(\mathcal{L}_\Gamma p_{n,l}^{k,i} + g_{n,l}^{k,i},\ \xi_{n,l} \right)_\Gamma = \left(q_{n,l}^{k,\theta},\ \xi_{n,l} \right)_{\Omega_l}, \tag{3.12}$$

$$\phi_l \left(\tfrac{s_l^{k,i} - s_l^{k-1}}{\Delta t},\ \xi_{w,l} \right)_{\Omega_l} - \left(\boldsymbol{u}_{w,l}^{k,\theta,i},\ \nabla \xi_{w,l} \right)_{\Omega_l} + \left(\mathcal{L}_\Gamma p_{w,l}^{k,i} + g_{w,l}^{k,i},\ \xi_{w,l} \right)_\Gamma = \left(q_{w,l}^{k,\theta},\ \xi_{w,l} \right)_{\Omega_l}, \tag{3.13}$$

$$g_{\alpha,l}^{k,i} = -2\mathcal{L}_\Gamma p_{\alpha,3-l}^{k,i-1} - g_{\alpha,3-l}^{k,i-1} \quad \text{in } L^2(\Gamma). \tag{3.14}$$

If the limit exists, we expect for (3.12)–(3.14) to iteratively find the solution of the formal limit system (3.8)–(3.10) as $i \to \infty$. Although this convergence is independent of the initial guess, as shown below in Theorems 4.1 and 4.2, note that the natural choice for the first iteration is the solutions of the previous time step, i.e.

$$s_l^{k,0} = s_l^{k-1}, \qquad p_{\alpha,l}^{k,0} = p_{\alpha,l}^{k-1}, \qquad g_{\alpha,l}^{k,0} = g_{\alpha,l}^{k-1}.$$

Note that the Robin condition formulated in (3.14) removes the necessity to calculate the fluxes at the interface Γ in favor of evaluating the pressure. This has the advantage that the regularity can be improved ($g_{\alpha,l}^{k,i} \in L^2(\Gamma)$ instead of $\boldsymbol{u}_{\alpha,l}^{k,\theta,i} \cdot \boldsymbol{\nu}_l \in H_{00}^{1/2}(\Gamma)'$) and that no post-processing is required for finite element methods and other pressure-based spatial discretization schemes.

For Problem 1, we use the stabilization parameters $\mathcal{L}_{p,l}, \mathcal{L}_{\Phi,l}, \mathcal{L}_{T,l} \geq 0$, which must satisfy some mild constraints to guarantee convergence, as shown below in Theorem 4.1. With these, the stabilized linearization of (3.4) becomes

$$\begin{aligned} p_{n,l}^{k,\theta,i} - p_{w,l}^{k,\theta,i} + \left(\mathcal{L}_{p,l} + \tfrac{\mathcal{L}_{T,l}+\mathcal{L}_{\Phi,l}}{\Delta t}\right)\left(s_l^{k,i} - s_l^{k,i-1}\right) \\ = \theta p_{c,l}(s_l^{k,i-1}) + (1-\theta)p_{c,l}^{k-1} - \Phi_{\delta,l}\left(\tfrac{s_l^{k,i-1}-s_l^{k-1}}{\Delta t}\right) - \tfrac{T_l(s_l^{k,i-1})-T_l(s_l^{k-1})}{\Delta t} \quad \text{in } L^2(\Omega_l), \end{aligned} \tag{3.15}$$

for $l \in \{1,2\}$, where $p_{\alpha,l}^{k,\theta,i} := \theta p_{\alpha,l}^{k,i} + (1-\theta)p_{\alpha,l}^{k-1}$. Clearly, the stabilizing term in (3.15) vanishes in the case of convergence, and hence the formal limit is (3.4). The iteration reduces to solving the following problem.

Problem LDD-1 (*Weak Formulation of the LDD-scheme I*)**.** Given $(s^{k-1}, p_n^{k-1}, p_w^{k-1}) \in \mathcal{V}$, $(s^{k,i-1}, p_n^{k,i-1}, p_w^{k,i-1}) \in \mathcal{W}$ and $g_{\alpha,l}^{k,i-1} \in L^2(\Gamma)$ for $l \in \{1,2\}$, $\alpha \in \{n,w\}$, find $(s^{k,i}, p_n^{k,i}, p_w^{k,i}) \in \mathcal{W}$ and $g_{\alpha,l}^{k,i} \in L^2(\Gamma)$ for $l \in \{1,2\}$ and $\alpha \in \{n,w\}$, such that Eqs. (3.12)–(3.15) hold for all $\xi_{n,l}, \xi_{w,l} \in \mathcal{W}_l$ and $l \in \{1,2\}$.

For Problem 2, we define the semi-linearized inverted capillary pressure equation based on (3.5) and $\Psi_l^{k,i} := \Psi_l(p_{n,l}^{k,i-1} - p_{w,l}^{k,i-1} - p_{c,l}(s_l^{k,i}))$ by

$$\tfrac{s_l^{k,i}-s_l^{k-1}}{\Delta t} = \theta\,\Psi_l^{k,i} + (1-\theta)\,\Psi_l^{k-1} \quad \text{in } L^2(\Omega_l) \text{ for } l \in \{1,2\}. \tag{3.16}$$

Note that $s_l^{k,i}$ still arises implicitly. However, (3.16) defines a contraction, as shown in Lemma 4.2. Therefore, it can be easily solved by directly applying the associated fixed-point iteration or any other suited method such as the Newton–Raphson iteration.

Note that this allows to use $s_l^{k,i}$ for the definition of the flux

$$\boldsymbol{u}_{\alpha,l}^{k,\theta,i} := -\theta\lambda_{\alpha,l}(s_l^{k,i})K_l\nabla p_{\alpha,l}^{k,i} + (1-\theta)\boldsymbol{u}_{\alpha,l}^{k-1}$$

in the second LDD-scheme. Substitution of (3.16) into (3.12) and (3.13) leads then to a nonlinear elliptic system of equations in $p_{n,l}$ and $p_{w,l}$. Therefore, we stabilize these equations using only one stabilization parameter $\mathcal{L}_{p,l} > 0$, which again must satisfy a mild constraint discussed in Section 4.2. In particular, the term $\mathcal{L}_{p,l}\big(p_{n,l}^{k,i} - p_{n,l}^{k,i-1} - p_{w,l}^{k,i} + p_{w,l}^{k,i-1}\big)$ is added to (3.12) and subtracted from (3.13). Again, this term vanishes in case of convergence. Altogether, the second LDD-scheme is constituted by iteratively solving the following problem.

Problem LDD-2 (*Weak Formulation of the LDD-scheme II*)**.** Given $(s^{k-1}, p_n^{k-1}, p_w^{k-1}) \in \mathcal{V}$, $(s^{k,i-1}, p_n^{k,i-1}, p_w^{k,i-1}) \in \mathcal{W}$ and $g_{\alpha,l}^{k,i-1} \in L^2(\Gamma)$ for $l \in \{1,2\}$, $\alpha \in \{n,w\}$, find $(s^{k,i}, p_n^{k,i}, p_w^{k,i}) \in \mathcal{W}$ and $g_{\alpha,l}^{k,i} \in L^2(\Gamma)$ for $l \in \{1,2\}$, $\alpha \in \{n,w\}$, such that it holds

$$\begin{aligned} -\phi_l\left(\tfrac{s_l^{k,i}-s_l^{k-1}}{\Delta t},\ \xi_{n,l}\right)_{\Omega_l} + \mathcal{L}_{p,l}\left(p_{n,l}^{k,i} - p_{n,l}^{k,i-1} - p_{w,l}^{k,i} + p_{w,l}^{k,i-1},\ \xi_{n,l}\right)_{\Omega_l} \\ - \left(\boldsymbol{u}_{n,l}^{k,\theta,i},\ \nabla\xi_{n,l}\right)_{\Omega_l} + \left(\mathcal{L}_\Gamma p_{n,l}^{k,i} + g_{n,l}^{k,i},\ \xi_{n,l}\right)_\Gamma = \left(q_{n,l}^{k,\theta},\ \xi_{n,l}\right)_{\Omega_l}, \end{aligned} \tag{3.17}$$

$$\begin{aligned} \phi_l\left(\tfrac{s_l^{k,i}-s_l^{k-1}}{\Delta t},\ \xi_{w,l}\right)_{\Omega_l} - \mathcal{L}_{p,l}\left(p_{n,l}^{k,i} - p_{n,l}^{k,i-1} - p_{w,l}^{k,i} + p_{w,l}^{k,i-1},\ \xi_{w,l}\right)_{\Omega_l} \\ - \left(\boldsymbol{u}_{w,l}^{k,\theta,i},\ \nabla\xi_{w,l}\right)_{\Omega_l} + \left(\mathcal{L}_\Gamma p_{w,l}^{k,i} + g_{w,l}^{k,i},\ \xi_{w,l}\right)_\Gamma = \left(q_{w,l}^{k,\theta},\ \xi_{w,l}\right)_{\Omega_l}, \end{aligned} \tag{3.18}$$

$$g_{\alpha,l}^{k,i} = -2\mathcal{L}_\Gamma p_{\alpha,3-l}^{k,i-1} - g_{\alpha,3-l}^{i-1} \quad \text{in } L^2(\Gamma), \tag{3.19}$$

$$\tfrac{s_l^{k,i}-s_l^{k-1}}{\Delta t} = \theta\,\Psi_l^{k,i} + (1-\theta)\,\Psi_l^{k-1} \quad \text{in } L^2(\Omega_l), \tag{3.20}$$

for all $\xi_{n,l}, \xi_{w,l} \in \mathcal{W}_l$ and $l \in \{1,2\}$.

4. Existence and convergence of the solutions to the LDD-schemes

In the following, Problems LDD-1 and LDD-2 defining the LDD-schemes are analyzed. The existence of unique solutions to these problems and the convergence towards the solutions of the semi-discrete equations is rigorously proven. The ideas of the proofs are based on [5,22,23], where similar models are discussed, in which either hysteresis or both dynamic capillarity and hysteresis are absent. In comparison to [25], the proofs are generalized and corrected. The LDD-scheme I is presented first, the second one afterwards.

4.1. Existence and convergence of the solutions to the LDD-scheme I

The existence of a unique solution to Problem LDD-1 is a direct consequence of the linearization.

Lemma 4.1. *Problem* LDD-1 *has a unique solution if Assumption 1 is fulfilled and* $\theta \in (0, 1]$.

Proof. Since $p_{\alpha,l}^{k,i-1}|_\Gamma \in L^2(\Gamma)$, (3.14) yields unique $g_{\alpha,l}^{k,i} \in L^2(\Gamma)$ for $l \in \{1,2\}$ and $\alpha \in \{n, w\}$. Further, (3.15) can be rewritten as

$$\frac{s_l^{k,i}-s_l^{k-1}}{\Delta t} = -\beta_l\theta\left(p_{n,l}^{k,i} - p_{w,l}^{k,i}\right) + \beta_l f_l^i \quad \text{in } L^2(\Omega_l), \tag{4.1}$$

where $\beta_l = (\mathcal{L}_{p,l}\Delta t + \mathcal{L}_{T,l} + \mathcal{L}_{\Phi,l})^{-1} > 0$, and

$$f_l^i = \theta p_{c,l}(s_l^{k,i-1}) + (1-\theta)p_{c,l}^{k-1} - (1-\theta)\left(p_{n,l}^{k-1} - p_{w,l}^{k-1}\right) - \Phi_{\delta,l}\left(\tfrac{s_l^{k,i-1}-s_l^{k-1}}{\Delta t}\right) - \tfrac{T_l(s_l^{k,i-1})-T_l(s_l^{k-1})}{\Delta t}$$

is independent of any quantity at the iteration i. Inserting this into the sum of (3.12) and (3.13) leads to

$$\begin{aligned}
&\phi_l\beta_l\theta\left(p_{n,l}^{k,i} - p_{w,l}^{k,i},\ \xi_{n,l} - \xi_{w,l}\right)_{\Omega_l} + \theta\sum_{\alpha\in\{n,w\}}\left(\lambda_{\alpha,l}(s_l^{k,i-1})K_l\nabla p_{\alpha,l}^{k,i},\ \nabla\xi_{\alpha,l}\right)_{\Omega_l} + \sum_{\alpha\in\{n,w\}}\mathcal{L}_\Gamma\left(p_{\alpha,l}^{k,i},\ \xi_{\alpha,l}\right)_\Gamma \\
&\quad = \phi_l\beta_l\left(f_l^i,\ \xi_{n,l} - \xi_{w,l}\right)_{\Omega_l} + (1-\theta)\sum_{\alpha\in\{n,w\}}\left(\boldsymbol{u}_{\alpha,l}^{k-1},\ \nabla\xi_{\alpha,l}\right)_{\Omega_l} + \sum_{\alpha\in\{n,w\}}\left(q_{\alpha,l}^{k,\theta},\ \xi_{\alpha,l}\right)_{\Omega_l} \\
&\qquad - \sum_{\alpha\in\{n,w\}}\left(g_{\alpha,l}^{k,i},\ \xi_{\alpha,l}\right)_\Gamma.
\end{aligned}$$

Note that the righthand side is independent of any quantity at iteration i except the known $g_{\alpha,l}^{k,i}$ in the last term. With respect to the product space $[\mathcal{W}_l]^2$, the first term on the lefthand side is positive semi-definite. The remaining terms of the lefthand side are a symmetric, coercive and continuous bilinear form on $[\mathcal{W}_l]^2$ by Assumption 1, $\theta > 0$ and $\mathcal{L}_\Gamma > 0$. The righthand side is a continuous linear functional on $[\mathcal{W}_l]^2$, hence by the Lax–Milgram lemma, a unique solution $(p_{n,l}^{k,i}, p_{w,l}^{k,i}) \in [\mathcal{W}_l]^2$ exists for $l \in \{1,2\}$. Finally, $s_l^{k,i} \in L^2(\Omega_l)$ is uniquely determined by (4.1). □

To prove the convergence of the LDD-scheme I, we derive a-priori estimates for the errors between the solution to Problem LDD-1 and the solution of the limit equations. These estimates yield the convergence for any initial guess.

Theorem 4.1 (*Convergence of the LDD-scheme I*)**.** *Let Assumption 1 be fulfilled and* $\theta \in (0, 1]$. *Assume that a solution* $(s^k, p_n^k, p_w^k) \in \mathcal{V}$ *of Problem 1 exists and satisfies* $\left\|K_l^{1/2}\nabla p_{\alpha,l}^k\right\|_{L^\infty(\Omega_l)} \le M_{p_\alpha,l}$ *and* $\boldsymbol{u}_{\alpha,l}^{k,\theta}\cdot\boldsymbol{\nu}_l \in L^2(\Gamma)$. *If the stabilization parameters are sufficiently large and the time step is small enough, i.e.*

$$\mathcal{L}_{p,l} \ge \theta L_{p_c,l}, \qquad \mathcal{L}_{T,l} \ge \frac{L_{T,l}}{2}, \qquad \mathcal{L}_{\Phi,l} \ge \frac{L_{\Phi_\delta,l}}{2} \qquad \text{and} \qquad \Delta t < \phi_l m_{p_c,l}\left(\sum_{\alpha\in\{n,w\}}\frac{\theta L_{\lambda_\alpha,l}^2 M_{p_\alpha,l}^2}{m_{\lambda_\alpha,l}}\right)^{-1},$$

for $l \in \{1,2\}$, *the sequence of solutions of Problem* LDD-1 *converges towards the solution of Problem 1 independently of the initial guess* $(s^{k,0}, p_n^{k,0}, p_w^{k,0}) \in \mathcal{W}$ *and* $g_{\alpha,l}^{k,0} \in L^2(\Gamma)$ *for* $l \in \{1,2\}$ *and* $\alpha \in \{n, w\}$. *More precisely, it holds*

$$s_l^{k,i} \to s_l^k \ \text{ in } \ L^2(\Omega_l), \qquad p_{\alpha,l}^{k,i} \to p_{\alpha,l}^k \ \text{ in } \ \mathcal{W}_l, \qquad g_{\alpha,l}^{k,i} \rightharpoonup g_{\alpha,l}^k \ \text{ in } \ L^2(\Gamma)$$

for $l \in \{1,2\}$ *and* $\alpha \in \{n, w\}$ *as* $i \to \infty$.

Remark 4.1. Due to the regularized sign-function, one has $L_{\Phi_\delta,l} = M_{\gamma,l}/\delta$. This means that the stabilization parameters and the time step can be chosen independently of the regularization, except for $\mathcal{L}_{\Phi,l} \geq M_{\gamma,l}/(2\delta)$.

Remark 4.2. Note that we assume the solution of the semi-discrete Problem 1 to exist and to be sufficiently smooth. Given the additional regularity assumptions mentioned in Remark 2.5, this holds for the continuous problem. In particular, following the proof of Lemma 1 in [50], the same arguments yield $s_l^k \in C^0(\overline{\Omega_l})$ and $p_{\alpha,l}^k \in C^1(\overline{\Omega_l})$ in the semi-discrete case under these assumptions. Then, one would have $\boldsymbol{u}_{\alpha,l}^{k,\theta} \in C^0(\overline{\Omega_l})$ and hence the regularity assumptions would be fulfilled. However, this remains an open problem if only Assumption 1 is fulfilled. Furthermore, the existence of the semi-discrete solutions remains unclear in both cases.

Proof of Theorem 4.1. The iteration errors are defined by

$$e_{s,l}^i := s_l^{k,i} - s_l^k \in L^2(\Omega_l), \qquad e_{p_\alpha,l}^i := p_{\alpha,l}^{k,i} - p_{\alpha,l}^k \in \mathcal{W}_l, \qquad e_{g_\alpha,l}^i := g_{\alpha,l}^{k,i} - g_{\alpha,l}^k \in L^2(\Gamma).$$

Subtraction of the limit equations (3.8), (3.9), (3.10) and (3.4) from (3.12)–(3.15) leads to

$$-\phi_l \left(\tfrac{e_{s,l}^i}{\Delta t},\ \xi_{n,l}\right)_{\Omega_l} + \theta \left(\lambda_{n,l}(s_l^{k,i-1}) K_l \nabla p_{n,l}^{k,i} - \lambda_{n,l}(s_l^k) K_l \nabla p_{n,l}^k,\ \nabla \xi_{n,l}\right)_{\Omega_l} + \left(\mathcal{L}_\Gamma e_{p_n,l}^i + e_{g_n,l}^i,\ \xi_{n,l}\right)_\Gamma = 0, \tag{4.2}$$

$$\phi_l \left(\tfrac{e_{s,l}^i}{\Delta t},\ \xi_{w,l}\right)_{\Omega_l} + \theta \left(\lambda_{w,l}(s_l^{k,i-1}) K_l \nabla p_{w,l}^{k,i} - \lambda_{w,l}(s_l^k) K_l \nabla p_{w,l}^k,\ \nabla \xi_{w,l}\right)_{\Omega_l} + \left(\mathcal{L}_\Gamma e_{p_w,l}^i + e_{g_w,l}^i,\ \xi_{w,l}\right)_\Gamma = 0, \tag{4.3}$$

$$e_{g_\alpha,l}^i = -2\mathcal{L}_\Gamma e_{p_\alpha,3-l}^{i-1} - e_{g_\alpha,3-l}^{i-1} \quad \text{in } L^2(\Gamma), \tag{4.4}$$

$$\begin{aligned} \theta\left(e_{p_n,l}^i - e_{p_w,l}^i\right) + \left(\mathcal{L}_{p,l} + \tfrac{\mathcal{L}_{T,l}+\mathcal{L}_{\Phi,l}}{\Delta t}\right)\left(e_{s,l}^i - e_{s,l}^{i-1}\right) \\ = \theta\left(p_{c,l}(s_l^{k,i-1}) - p_{c,l}(s_l^k)\right) - \tfrac{T_l(s_l^{k,i-1}) - T_l(s_l^k)}{\Delta t} \\ - \left(\Phi_{\delta,l}\left(\tfrac{s_l^{k,i-1} - s_l^{k-1}}{\Delta t}\right) - \Phi_{\delta,l}\left(\tfrac{s_l^k - s_l^{k-1}}{\Delta t}\right)\right) \quad \text{in } L^2(\Omega_l). \end{aligned} \tag{4.5}$$

In the following, we derive estimates for the errors at iteration i depending on those of the previous iteration $i-1$. This is done separately for each of Eqs. (4.2)–(4.5) using the monotonicity of the coefficient functions. Combining these estimates, we observe absolute convergence of the series of errors, and conclude the convergence of the solution.

Error estimate on the interface conditions. Using (4.4), the norm of $e_{g_\alpha,l}^i$ is

$$\left\|e_{g_\alpha,l}^i\right\|_\Gamma^2 = 4\mathcal{L}_\Gamma \left(\mathcal{L}_\Gamma e_{p_\alpha,3-l}^{i-1} + e_{g_\alpha,3-l}^{i-1},\ e_{p_\alpha,3-l}^{i-1}\right)_\Gamma + \left\|e_{g_\alpha,3-l}^{i-1}\right\|_\Gamma^2$$

and thus by index shifting i to $i+1$ and l to $3-l$

$$\left(\mathcal{L}_\Gamma e_{p_\alpha,l}^i + e_{g_\alpha,l}^i,\ e_{p_\alpha,l}^i\right)_\Gamma = -\frac{1}{4\mathcal{L}_\Gamma}\left(\left\|e_{g_\alpha,l}^i\right\|_\Gamma^2 - \left\|e_{g_\alpha,3-l}^{i+1}\right\|_\Gamma^2\right). \tag{4.6}$$

Error estimate on the non-wetting pressure. Testing (4.2) with $\xi_{n,l} = e_{p_n,l}^i$ yields

$$\begin{aligned} -\phi_l \left(\tfrac{e_{s,l}^i}{\Delta t},\ e_{p_n,l}^i\right)_{\Omega_l} + \theta \left(\lambda_{n,l}(s_l^{k,i-1}) K_l \nabla e_{p_n,l}^i,\ \nabla e_{p_n,l}^i\right)_{\Omega_l} + \left(\mathcal{L}_\Gamma e_{p_n,l}^i + e_{g_n,l}^i,\ e_{p_n,l}^i\right)_\Gamma \\ + \theta \left(\left(\lambda_{n,l}(s_l^{k,i-1}) - \lambda_{n,l}(s_l^k)\right) K_l \nabla p_{n,l}^k,\ \nabla e_{p_n,l}^i\right)_{\Omega_l} = 0. \end{aligned}$$

Since $\lambda_{n,l}$ has the lower bound $m_{\lambda_n,l}$ and is Lipschitz continuous, one obtains by the Cauchy–Schwarz inequality and (4.6)

$$\begin{aligned} -\phi_l \left(\tfrac{e_{s,l}^i}{\Delta t},\ e_{p_n,l}^i\right)_{\Omega_l} + \theta m_{\lambda_n,l} \left\|K_l^{1/2} \nabla e_{p_n,l}^i\right\|_{\Omega_l}^2 - \tfrac{1}{4\mathcal{L}_\Gamma}\left(\left\|e_{g_\alpha,l}^i\right\|_\Gamma^2 - \left\|e_{g_\alpha,3-l}^{i+1}\right\|_\Gamma^2\right) \\ \leq \theta L_{\lambda_n,l} \left\|K_l^{1/2} \nabla p_{n,l}^k\right\|_{L^\infty(\Omega_l)} \left\|e_{s,l}^{i-1}\right\|_{\Omega_l} \left\|K_l^{1/2} \nabla e_{p_n,l}^i\right\|_{\Omega_l}. \end{aligned}$$

By Young's inequality and the bound on the pressure gradient, one gets

$$-\phi_l\left(\frac{e^i_{s,l}}{\Delta t},\ e^i_{p_n,l}\right)_{\Omega_l}+\frac{\theta m_{\lambda_n,l}}{2}\left\|K_l^{1/2}\nabla e^i_{p_n,l}\right\|^2_{\Omega_l}\leq\frac{\theta L^2_{\lambda_n,l}M^2_{p_n,l}}{2m_{\lambda_n,l}}\left\|e^{i-1}_{s,l}\right\|^2_{\Omega_l}+\frac{1}{4\mathcal{L}_\Gamma}\left(\left\|e^i_{g_\alpha,l}\right\|^2_\Gamma-\left\|e^{i+1}_{g_\alpha,3-l}\right\|^2_\Gamma\right). \tag{4.7}$$

Error estimate on the wetting pressure. Testing (4.3) with $\xi_{w,l}=e^i_{p_w,l}$ and following the same steps as for the non-wetting pressure equation yields

$$\phi_l\left(\frac{e^i_{s,l}}{\Delta t},\ e^i_{p_w,l}\right)_{\Omega_l}+\frac{\theta m_{\lambda_w,l}}{2}\left\|K_l^{1/2}\nabla e^i_{p_w,l}\right\|^2_{\Omega_l}\leq\frac{\theta L^2_{\lambda_w,l}M^2_{p_w,l}}{2m_{\lambda_w,l}}\left\|e^{i-1}_{s,l}\right\|^2_{\Omega_l}+\frac{1}{4\mathcal{L}_\Gamma}\left(\left\|e^i_{g_w,l}\right\|^2_\Gamma-\left\|e^{i+1}_{g_w,3-l}\right\|^2_\Gamma\right). \tag{4.8}$$

Error estimate on the pressure difference. Testing (4.5) with $e^i_{s,l}$ and using the identity $a(a-b)=\frac{1}{2}(a^2-b^2+(a-b)^2)$ for the stabilization term yields

$$\begin{aligned}
&\theta\left(e^i_{p_n,l}-e^i_{p_w,l},\ e^i_{s,l}\right)_{\Omega_l}+\left(\frac{\mathcal{L}_{p,l}}{2}+\frac{\mathcal{L}_{T,l}+\mathcal{L}_{\Phi,l}}{2\Delta t}\right)\left(\left\|e^i_{s,l}\right\|^2_{\Omega_l}-\left\|e^{i-1}_{s,l}\right\|^2_{\Omega_l}+\left\|e^i_{s,l}-e^{i-1}_{s,l}\right\|^2_{\Omega_l}\right)\\
&=\left(\theta\left(p_{c,l}(s_l^{k,i-1})-p_{c,l}(s_l^k)\right)-\frac{T_l(s_l^{k,i-1})-T_l(s_l^k)}{\Delta t}-\left(\Phi_{\delta,l}\left(\frac{s_l^{k,i-1}-s_l^{k-1}}{\Delta t}\right)-\Phi_{\delta,l}\left(\frac{s_l^k-s_l^{k-1}}{\Delta t}\right)\right),\ e^{i-1}_{s,l}\right)_{\Omega_l}\\
&\quad+\left(\theta\left(p_{c,l}(s_l^{k,i-1})-p_{c,l}(s_l^k)\right)-\frac{T_l(s_l^{k,i-1})-T_l(s_l^k)}{\Delta t},\ e^i_{s,l}-e^{i-1}_{s,l}\right)_{\Omega_l}\\
&\quad-\left(\Phi_{\delta,l}\left(\frac{s_l^{k,i-1}-s_l^{k-1}}{\Delta t}\right)-\Phi_{\delta,l}\left(\frac{s_l^k-s_l^{k-1}}{\Delta t}\right),\ e^i_{s,l}-e^{i-1}_{s,l}\right)_{\Omega_l}.
\end{aligned}$$

The last two terms on the righthand side can be bounded by Cauchy–Schwarz inequality and Young's inequality, which yields

$$\begin{aligned}
&\theta\left(e^i_{p_n,l}-e^i_{p_w,l},\ e^i_{s,l}\right)_{\Omega_l}+\left(\frac{\mathcal{L}_{p,l}}{2}+\frac{\mathcal{L}_{T,l}+\mathcal{L}_{\Phi,l}}{2\Delta t}\right)\left(\left\|e^i_{s,l}\right\|^2_{\Omega_l}-\left\|e^{i-1}_{s,l}\right\|^2_{\Omega_l}\right)\\
&\leq\left(\theta\left(p_{c,l}(s_l^{k,i-1})-p_{c,l}(s_l^k)\right)-\frac{T_l(s_l^{k,i-1})-T_l(s_l^k)}{\Delta t}-\left(\Phi_{\delta,l}\left(\frac{s_l^{k,i-1}-s_l^{k-1}}{\Delta t}\right)-\Phi_{\delta,l}\left(\frac{s_l^k-s_l^{k-1}}{\Delta t}\right)\right),\ e^{i-1}_{s,l}\right)_{\Omega_l}\\
&\quad+\frac{\theta^2}{2\mathcal{L}_{p,l}}\left\|p_{c,l}(s_l^{k,i-1})-p_{c,l}(s_l^k)\right\|^2_{\Omega_l}+\frac{\Delta t}{2\mathcal{L}_{T,l}}\left\|\frac{T_l(s_l^{k,i-1})-T_l(s_l^k)}{\Delta t}\right\|^2_{\Omega_l}\\
&\quad+\frac{\Delta t}{2\mathcal{L}_{\Phi,l}}\left\|\Phi_{\delta,l}\left(\frac{s_l^{k,i-1}-s_l^{k-1}}{\Delta t}\right)-\Phi_{\delta,l}\left(\frac{s_l^k-s_l^{k-1}}{\Delta t}\right)\right\|^2_{\Omega_l}.
\end{aligned}$$

For a Lipschitz-continuous and monotonically increasing function $f:\mathbb{R}\to\mathbb{R}$, it holds $(f(a)-f(b))(a-b)\geq\frac{1}{L_f}|f(a)-f(b)|^2$ for all $a,b\in\mathbb{R}$, where L_f denotes the Lipschitz constant of f. Since $p_{c,l}$, T_l and $\Phi_{\delta,l}$ are Lipschitz-continuous and monotone, one thereby gets

$$\begin{aligned}
&\theta\left(e^i_{p_n,l}-e^i_{p_w,l},\ e^i_{s,l}\right)_{\Omega_l}+\left(\frac{\mathcal{L}_{p,l}}{2}+\frac{\mathcal{L}_{T,l}+\mathcal{L}_{\Phi,l}}{2\Delta t}\right)\left(\left\|e^i_{s,l}\right\|^2_{\Omega_l}-\left\|e^{i-1}_{s,l}\right\|^2_{\Omega_l}\right)+\frac{\theta}{2}\left(\left|p_{c,l}(s_l^{k,i-1})-p_{c,l}(s_l^k)\right|,\ \left|e^{i-1}_{s,l}\right|\right)_{\Omega_l}\\
&\leq\left(\frac{\theta^2}{2\mathcal{L}_{p,l}}-\frac{\theta}{2L_{p_c,l}}\right)\left\|p_{c,l}(s_l^{k,i-1})-p_{c,l}(s_l^k)\right\|^2_{\Omega_l}+\left(\frac{\Delta t}{2\mathcal{L}_{T,l}}-\frac{\Delta t}{L_{T,l}}\right)\left\|\frac{T_l(s_l^{k,i-1})-T_l(s_l^k)}{\Delta t}\right\|^2_{\Omega_l}\\
&\quad+\left(\frac{\Delta t}{2\mathcal{L}_{\Phi,l}}-\frac{\Delta t}{L_{\Phi_\delta,l}}\right)\left\|\Phi_{\delta,l}\left(\frac{s_l^{k,i-1}-s_l^{k-1}}{\Delta t}\right)-\Phi_{\delta,l}\left(\frac{s_l^k-s_l^{k-1}}{\Delta t}\right)\right\|^2_{\Omega_l}.
\end{aligned}$$

Since $\mathcal{L}_{p,l}\geq\theta L_{p_c,l}$, $\mathcal{L}_{T,l}\geq L_{T,l}/2$ and $\mathcal{L}_{\Phi,l}\geq L_{\Phi_\delta,l}/2$ by assumption, the terms on the righthand side can be neglected. Furthermore, using the lower bound $m_{p_c,l}\left|s_l^{k,i-1}-s_l^k\right|\leq\left|p_{c,l}(s_l^{k,i-1})-p_{c,l}(s_l^k)\right|$ from Assumption 1, one obtains

$$\theta\left(e^i_{p_n,l}-e^i_{p_w,l},\ e^i_{s,l}\right)_{\Omega_l}+\left(\frac{\mathcal{L}_{p,l}}{2}+\frac{\mathcal{L}_{T,l}+\mathcal{L}_{\Phi,l}}{2\Delta t}\right)\left(\left\|e^i_{s,l}\right\|^2_{\Omega_l}-\left\|e^{i-1}_{s,l}\right\|^2_{\Omega_l}\right)+\frac{\theta m_{p_c,l}}{2}\left\|e^{i-1}_{s,l}\right\|^2_{\Omega_l}\leq 0.$$

Multiplication with $\phi_l(\theta\Delta t)^{-1}$ finally leads to

$$\phi_l\left(e^i_{p_n,l}-e^i_{p_w,l},\ \frac{e^i_{s,l}}{\Delta t}\right)_{\Omega_l}+\frac{\phi_l m_{p_c,l}}{2\Delta t}\left\|e^{i-1}_{s,l}\right\|^2_{\Omega_l}\leq\frac{\phi_l}{\theta\Delta t}\left(\frac{\mathcal{L}_{p,l}}{2}+\frac{\mathcal{L}_{T,l}+\mathcal{L}_{\Phi,l}}{2\Delta t}\right)\left(\left\|e^{i-1}_{s,l}\right\|^2_{\Omega_l}-\left\|e^i_{s,l}\right\|^2_{\Omega_l}\right). \tag{4.9}$$

Combined error estimate. Summation of the estimates (4.7)–(4.9) yields

$$\sum_{\alpha\in\{n,w\}} \tfrac{\theta m_{\lambda_\alpha,l}}{2}\left\| K_l^{1/2}\nabla e^i_{p_\alpha,l}\right\|^2_{\Omega_l} + C_l(\Delta t)\left\| e^{i-1}_{s,l}\right\|^2_{\Omega_l}$$
$$\leq \tfrac{1}{4\mathcal{L}_\Gamma}\sum_{\alpha\in\{n,w\}}\left(\left\| e^i_{g_\alpha,l}\right\|^2_\Gamma - \left\| e^{i+1}_{g_\alpha,3-l}\right\|^2_\Gamma\right) + \tfrac{\phi_l}{\theta\Delta t}\left(\tfrac{\mathcal{L}_{p,l}}{2} + \tfrac{\mathcal{L}_{T,l}+\mathcal{L}_{\Phi,l}}{2\Delta t}\right)\left(\left\| e^{i-1}_{s,l}\right\|^2_{\Omega_l} - \left\| e^i_{s,l}\right\|^2_{\Omega_l}\right),$$

where by assumption

$$C_l(\Delta t) = \tfrac{\phi_l m_{p_c,l}}{2\Delta t} - \sum_{\alpha\in\{n,w\}} \tfrac{\theta L^2_{\lambda_\alpha,l} M^2_{p_\alpha,l}}{2m_{\lambda_\alpha,l}} > 0.$$

By summing the estimates for $l\in\{1,2\}$ and $i = 1,2,\ldots,r$, one gets

$$\sum_{i=1}^{r}\sum_{l=1}^{2}\sum_{\alpha\in\{n,w\}} \tfrac{\theta m_{\lambda_\alpha,l}}{2}\left\| K_l^{1/2}\nabla e^i_{p_\alpha,l}\right\|^2_{\Omega_l} + \sum_{i=1}^{r}\sum_{l=1}^{2} C_l(\Delta t)\left\| e^{i-1}_{s,l}\right\|^2_{\Omega_l}$$
$$\leq \tfrac{1}{4\mathcal{L}_\Gamma}\sum_{l=1}^{2}\sum_{\alpha\in\{n,w\}}\left\| e^1_{g_\alpha,l}\right\|^2_\Gamma + \tfrac{\phi_l}{\theta\Delta t}\sum_{l=1}^{2}\left(\tfrac{\mathcal{L}_{p,l}}{2} + \tfrac{\mathcal{L}_{T,l}+\mathcal{L}_{\Phi,l}}{2\Delta t}\right)\left\| e^0_{s,l}\right\|^2_{\Omega_l}.$$

Since the righthand side is independent of r, we conclude that the series on the left are absolutely convergent. Therefore, $s^{k,i}_l \to s^k_l$ in $L^2(\Omega_l)$ and the Poincaré inequality implies $p^{k,i}_{\alpha,l} \to p^k_{\alpha,l}$ in $\mathcal{W}_l$. To show the convergence of the $g^{k,i}_{\alpha,l}$, we consider again (4.2) and (4.3), and take the limit $i\to\infty$. By continuity one obtains

$$\lim_{i\to\infty}\left(e^i_{g_\alpha,l},\ \xi_{\alpha,l}\right)_\Gamma = 0$$

for any $\xi_{\alpha,l}\in\mathcal{W}_l$. Since the trace operator is surjective onto $H^{1/2}_{00}(\Gamma)$, which is dense in $L^2(\Gamma)$, we conclude $e^i_{g_\alpha,l} \rightharpoonup 0$ in $L^2(\Gamma)$ as $i\to\infty$. Additionally, one can directly obtain $e^i_{g_\alpha,l} + e^{i-1}_{g_\alpha,3-l} \to 0$ in $L^2(\Gamma)$ by (4.4). □

4.2. Existence and convergence of the solutions to the LDD-scheme II

The existence of a unique solution to Problem LDD-2 is again a consequence of the linearization, but using additionally the contraction property in (3.20).

Lemma 4.2. *Problem* LDD-2 *has a unique solution if Assumption* 1 *is fulfilled,* $\theta\in(0,1]$*, and it holds* $\Delta t < \frac{1}{\theta L_{\Psi,l} L_{p_c,l}}$.

Proof. Since $p^{k,i-1}_{\alpha,l}|_\Gamma \in L^2(\Gamma)$, (3.14) uniquely provides $g^{k,i}_{\alpha,l}\in L^2(\Gamma)$ for $\alpha\in n, w$ and $l\in\{1,2\}$. After multiplying (3.20) by Δt and adding s^{k-1}_l, the lefthand side is $s^{k,i}_l$, while the righthand side, considered as function

$$F_l(s^{k,i}_l) := s^{k-1}_l + \Delta t\theta\,\Psi_l\left(p^{k,i-1}_{n,l} - p^{k,i-1}_{w,l} - p_{c,l}(s^{k,i}_l)\right) + \Delta t(1-\theta)\,\Psi^{k-1}_l, \tag{4.10}$$

maps $L^2(\Omega_l)$ into itself. Moreover, for $s, r\in L^2(\Omega_l)$, it holds

$$\left\| F_l(s) - F_l(r)\right\|_{\Omega_l} \leq \Delta t\theta L_{\Psi,l} L_{p_c,l}\left\| s - r\right\|_{\Omega_l}.$$

By assumption $\Delta t\theta L_{\Psi,l}L_{p_c,l} < 1$, so F_l is a contraction, and the Banach fixed-point theorem yields the existence of a unique solution $s^{k,i}_l\in L^2(\Omega_l)$ to (3.20). Reordering of the sum of (3.17) and (3.18) leads to

$$\mathcal{L}_{p,l}\left(p^{k,i}_{n,l} - p^{k,i}_{w,l},\ \xi_{n,l} - \xi_{w,l}\right)_{\Omega_l} + \theta\sum_{\alpha\in\{n,w\}}\left(\lambda_{\alpha,l}(s^{k,i}_l)K_l\nabla p^{k,i}_{\alpha,l},\ \nabla\xi_{\alpha,l}\right)_{\Omega_l} + \sum_{\alpha\in\{n,w\}}\mathcal{L}_\Gamma\left(p^{k,i}_{\alpha,l},\ \xi_{\alpha,l}\right)_\Gamma$$
$$= \sum_{\alpha\in\{n,w\}}\left(q^{k,\theta}_{\alpha,l},\ \xi_{\alpha,l}\right)_{\Omega_l} + (1-\theta)\sum_{\alpha\in\{n,w\}}\left(\boldsymbol{u}^{k,i-1}_{\alpha,l},\ \nabla\xi_{\alpha,l}\right)_{\Omega_l} + \mathcal{L}_{p,l}\left(p^{k,i-1}_{n,l} - p^{k,i-1}_{w,l},\ \xi_{n,l} - \xi_{w,l}\right)_{\Omega_l}$$
$$- \sum_{\alpha\in\{n,w\}}\left(g^{k,i}_{\alpha,l},\ \xi_{\alpha,l}\right)_\Gamma + \phi_l\left(\tfrac{s^{k,i}_l - s^{k-1}_l}{\Delta t},\ \xi_{n,l} - \xi_{w,l}\right)_{\Omega_l},$$

where the righthand side is independent of $p_{n,l}^{k,i}$ and $p_{w,l}^{k,i}$. As before for the first scheme, the first term on the lefthand side is positive semi-definite with respect to the product space $[\mathcal{W}_l]^2$, while the remaining terms of the lefthand side form a symmetric, coercive and continuous bilinear form on $[\mathcal{W}_l]^2$ by Assumption 1, $\theta > 0$ and $\mathcal{L}_\Gamma > 0$. The righthand side is a continuous linear functional on $[\mathcal{W}_l]^2$, hence by the Lax–Milgram lemma, a unique solution $(p_{n,l}^{k,i}, p_{w,l}^{k,i}) \in [\mathcal{W}_l]^2$ exists for $l \in \{1, 2\}$. □

To prove the convergence of the LDD-scheme II, we derive a-priori estimates for the errors between the solution to Problem LDD-2 and the solution of the limit equations. These estimates then yield the convergence for any initial guess.

Theorem 4.2 (*Convergence of the LDD-scheme II*)**.** *Let Assumption 1 be fulfilled, and let $\theta \in (0, 1]$ and $\tau_l > 0$ be fixed. Assume, that a solution $(s^k, p_n^k, p_w^k) \in \mathcal{V}$ of Problem 2 satisfying $\left\| K_l^{1/2} \nabla p_{\alpha,l}^k \right\|_{L^\infty(\Omega_l)} \leq M_{p_\alpha,l}$ and $\boldsymbol{u}_{\alpha,l}^{k,\theta} \cdot \boldsymbol{\nu}_l \in L^2(\Gamma)$ exists. If the stabilization parameter is sufficiently large and the time step is small enough, i.e.*

$$\mathcal{L}_{p,l} > 2\phi_l \theta L_{\Psi,l}, \qquad \Delta t \leq \frac{1}{2\theta L_{\Psi,l} L_{p_c,l}} \qquad \text{and} \qquad \Delta t \leq \sqrt{\frac{\frac{1}{2\theta\phi_l L_{\Psi,l}} - \frac{1}{\mathcal{L}_{p,l}}}{\sum_{\alpha\in\{n,w\}} \left(\frac{2\theta L_{\Psi,l}^2 L_{p_c,l}^2 C_{\Omega_l}^2}{m_{\lambda_\alpha,l} \underline{K}_l} + \frac{\theta L_{\lambda_\alpha,l}^2 M_{p_\alpha,l}^2}{\phi_l^2 m_{\lambda_\alpha,l}} \right)}}$$

for $l \in \{1, 2\}$, the sequence of solutions of Problem LDD-2 converges towards the solution of Problem 2 independently of the initial guess $(s^{k,0}, p_n^{k,0}, p_w^{k,0}) \in \mathcal{W}$ and $g_{\alpha,l}^{k,0} \in L^2(\Gamma)$ for $l \in \{1, 2\}$ and $\alpha \in \{n, w\}$. More precisely, it holds

$$s_l^{k,i} \to s_l^k \ \text{ in } \ L^2(\Omega_l), \qquad p_{\alpha,l}^{k,i} \to p_{\alpha,l}^k \ \text{ in } \ \mathcal{W}_l, \qquad g_{\alpha,l}^{k,i} \rightharpoonup g_{\alpha,l}^k \ \text{ in } \ L^2(\Gamma)$$

for $l \in \{1, 2\}$, $\alpha \in \{n, w\}$ as $i \to \infty$.

Proof. We define the iteration errors by

$$e_{s,l}^i := s_l^{k,i} - s_l^k \in L^2(\Omega_l), \qquad e_{p_\alpha,l}^i := p_{\alpha,l}^{k,i} - p_{\alpha,l}^k \in \mathcal{W}_l, \qquad e_{g_\alpha,l}^i := g_{\alpha,l}^{k,i} - g_{\alpha,l}^k \in L^2(\Gamma),$$
$$e_{p_c,l}^i := e_{p_n,l}^i - e_{p_w,l}^i \in \mathcal{W}_l, \qquad e_{\Psi,l}^i := \Psi_l^{k,i} - \Psi_l(p_{n,l}^k - p_{w,l}^k - p_{c,l}(s_l^{k,i})) \in L^2(\Gamma).$$

Subtracting the limit equations (3.8), (3.9), (3.10) and (3.5) from (3.17)–(3.20) gives

$$-\phi_l \left(\frac{e_{s,l}^i}{\Delta t}, \ \xi_{n,l} \right)_{\Omega_l} + \mathcal{L}_{p,l} \left(e_{p_c,l}^i - e_{p_c,l}^{i-1}, \ \xi_{n,l} \right)_{\Omega_l} - \left(\boldsymbol{u}_{n,l}^{k,\theta,i} - \boldsymbol{u}_{n,l}^{k,\theta}, \ \nabla \xi_{n,l} \right)_{\Omega_l} + \left(\mathcal{L}_\Gamma e_{p_n,l}^i + e_{g_n,l}^i, \ \xi_{n,l} \right)_\Gamma = 0, \tag{4.11}$$

$$\phi_l \left(\frac{e_{s,l}^i}{\Delta t}, \ \xi_{w,l} \right)_{\Omega_l} - \mathcal{L}_{p,l} \left(e_{p_c,l}^i - e_{p_c,l}^{i-1}, \ \xi_{w,l} \right)_{\Omega_l} - \left(\boldsymbol{u}_{w,l}^{k,\theta,i} - \boldsymbol{u}_{w,l}^{k,\theta}, \ \nabla \xi_{w,l} \right)_{\Omega_l} + \left(\mathcal{L}_\Gamma e_{p_w,l}^i + e_{g_w,l}^i, \ \xi_{w,l} \right)_\Gamma = 0, \tag{4.12}$$

$$e_{g_\alpha,l}^i = -2\mathcal{L}_\Gamma e_{p_\alpha,3-l}^{i-1} - e_{g_\alpha,3-l}^{i-1} \quad \text{in } L^2(\Gamma), \tag{4.13}$$

$$\frac{e_{s,l}^i}{\Delta t} = \theta \left(\Psi_l^{k,i} - \Psi_l^k \right) \quad \text{in } L^2(\Omega_l). \tag{4.14}$$

As for the proof of Theorem 4.1, we derive estimates for the errors at iteration i depending on those of the previous iteration $i-1$. This is done separately for (4.11), (4.12) and (4.14) using the monotonicity of the coefficient functions. For (4.13) we use the estimate (4.6) from the proof of Theorem 4.1. Combining the estimates, the convergence of the solution follows from the absolute convergence of the series of errors.

Error estimate on the saturation. Eq. (4.14) yields

$$\begin{aligned} \tfrac{1}{\Delta t} \left\| e_{s,l}^i \right\|_{\Omega_l} &= \theta \left\| \Psi_l^{k,i} - \Psi_l^k \right\|_{\Omega_l} \\ &\leq \theta \left\| \Psi_l^{k,i} - \Psi_l(p_{n,l}^k - p_{w,l}^k - p_{c,l}(s_l^{k,i})) \right\|_{\Omega_l} + \theta \left\| \Psi_l(p_{n,l}^k - p_{w,l}^k - p_{c,l}(s_l^{k,i})) - \Psi_l^k \right\|_{\Omega_l} \\ &\leq \theta \left\| e_{\Psi,l}^i \right\|_{\Omega_l} + \theta L_{\Psi,l} L_{p_c,l} \left\| e_{s_l}^i \right\|_{\Omega_l}. \end{aligned}$$

In the last step, the Lipschitz continuity of Ψ_l and $p_{c,l}$ is used. Multiplying by Δt and using $\Delta t \leq (2\theta L_{\Psi,l} L_{p_c,l})^{-1}$ yields

$$\left\| e^i_{s,l} \right\|_{\Omega_l} \leq 2\theta \Delta t \left\| e^i_{\Psi,l} \right\|_{\Omega_l}. \tag{4.15}$$

Error estimate on the non-wetting pressure. Note that (4.13) again leads to (4.6). Therefore, testing (4.11) with $\xi_{n,l} = e^i_{p_n,l}$ yields

$$\begin{aligned} -\phi_l \left(\tfrac{e^i_{s,l}}{\Delta t},\ e^i_{p_n,l} \right)_{\Omega_l} &+ \mathcal{L}_{p,l} \left(e^i_{p_c,l} - e^{i-1}_{p_c,l},\ e^i_{p_n,l} \right)_{\Omega_l} + \theta \left(\lambda_{n,l}(s^{k,i}_l) K_l \nabla e^i_{p_n,l},\ \nabla e^i_{p_n,l} \right)_{\Omega_l} \\ &= -\theta \left(\left(\lambda_{n,l}(s^{k,i}_l) - \lambda_{n,l}(s^k_l) \right) K_l \nabla p^k_{n,l},\ \nabla e^i_{p_n,l} \right)_{\Omega_l} + \tfrac{1}{4\mathcal{L}_\Gamma} \left(\left\| e^{i+1}_{g_n,l} \right\|^2_\Gamma - \left\| e^i_{g_n,3-l} \right\|^2_\Gamma \right). \end{aligned}$$

By the lower bound $m_{\lambda_n,l}$ on $\lambda_{n,l}$, the Lipschitz continuity of $\lambda_{n,l}$ and the bound on the pressure gradient, one obtains with the Cauchy–Schwarz inequality

$$\begin{aligned} -\phi_l \left(\tfrac{e^i_{s,l}}{\Delta t},\ e^i_{p_n,l} \right)_{\Omega_l} &+ \mathcal{L}_{p,l} \left(e^i_{p_c,l} - e^{i-1}_{p_c,l},\ e^i_{p_n,l} \right)_{\Omega_l} + \theta m_{\lambda_n,l} \left\| K_l^{1/2} \nabla e^i_{p_n,l} \right\|^2_{\Omega_l} \\ &\leq \theta L_{\lambda_n,l} M_{p_n,l} \left\| e^i_{s,l} \right\|_{\Omega_l} \left\| K^{1/2} \nabla e^i_{p_n,l} \right\|_{\Omega_l} + \tfrac{1}{4\mathcal{L}_\Gamma} \left(\left\| e^{i+1}_{g_n,l} \right\|^2_\Gamma - \left\| e^i_{g_n,3-l} \right\|^2_\Gamma \right). \end{aligned}$$

Young's inequality and estimate (4.15) lead to

$$\begin{aligned} -\phi_l \left(\tfrac{e^i_{s,l}}{\Delta t},\ e^i_{p_n,l} \right)_{\Omega_l} &+ \mathcal{L}_{p,l} \left(e^i_{p_c,l} - e^{i-1}_{p_c,l},\ e^i_{p_n,l} \right)_{\Omega_l} + \tfrac{\theta m_{\lambda_n,l}}{2} \left\| K_l^{1/2} \nabla e^i_{p_n,l} \right\|^2_{\Omega_l} \\ &\leq \tfrac{2\Delta t^2 \theta^3 L^2_{\lambda_n,l} M^2_{p_n,l}}{m_{\lambda_n,l}} \left\| e^i_{\Psi,l} \right\|^2_{\Omega_l} + \tfrac{1}{4\mathcal{L}_\Gamma} \left(\left\| e^{i+1}_{g_n,l} \right\|^2_\Gamma - \left\| e^i_{g_n,3-l} \right\|^2_\Gamma \right). \end{aligned} \tag{4.16}$$

Error estimate on the wetting pressure. Testing (4.3) with $\xi_{w,l} = e^i_{p_w,l}$ and following the same steps as for the non-wetting pressure equation yields

$$\begin{aligned} \phi_l \left(\tfrac{e^i_{s,l}}{\Delta t},\ e^i_{p_w,l} \right)_{\Omega_l} &- \mathcal{L}_{p,l} \left(e^i_{p_c,l} - e^{i-1}_{p_c,l},\ e^i_{p_w,l} \right)_{\Omega_l} + \tfrac{\theta m_{\lambda_w,l}}{2} \left\| K_l^{1/2} \nabla e^i_{p_w,l} \right\|^2_{\Omega_l} \\ &\leq \tfrac{2\Delta t^2 \theta^3 L^2_{\lambda_w,l} M^2_{p_w,l}}{m_{\lambda_w,l}} \left\| e^i_{\Psi,l} \right\|^2_{\Omega_l} + \tfrac{1}{4\mathcal{L}_\Gamma} \left(\left\| e^i_{g_w,l} \right\|^2_\Gamma - \left\| e^{i+1}_{g_w,3-l} \right\|^2_\Gamma \right). \end{aligned} \tag{4.17}$$

Combined error estimate. Addition of the pressure estimates (4.16) and (4.17) yields by the identity $(a-b)a = \frac{1}{2}(a^2 - b^2 + (a-b)^2)$

$$\begin{aligned} -\phi_l \left(\tfrac{e^i_{s,l}}{\Delta t},\ e^i_{p_c,l} \right)_{\Omega_l} &+ \tfrac{\mathcal{L}_{p,l}}{2} \left(\left\| e^i_{p_c,l} \right\|^2_{\Omega_l} - \left\| e^{i-1}_{p_c,l} \right\|^2_{\Omega_l} + \left\| e^i_{p_c,l} - e^{i-1}_{p_c,l} \right\|^2_{\Omega_l} \right) + \sum_{\alpha \in \{n,w\}} \tfrac{\theta m_{\lambda_\alpha,l}}{2} \left\| K_l^{1/2} \nabla e^i_{p_\alpha,l} \right\|^2_{\Omega_l} \\ &\leq \tfrac{1}{4\mathcal{L}_\Gamma} \sum_{\alpha \in \{n,w\}} \left(\left\| e^i_{g_\alpha,l} \right\|^2_\Gamma - \left\| e^{i+1}_{g_\alpha,3-l} \right\|^2_\Gamma \right) + \sum_{\alpha \in \{n,w\}} \tfrac{2\Delta t^2 \theta^3 L^2_{\lambda_\alpha,l} M^2_{p_\alpha,l}}{m_{\lambda_\alpha,l}} \left\| e^i_{\Psi,l} \right\|^2_{\Omega_l}. \end{aligned} \tag{4.18}$$

The first term on the lefthand side can be estimated as follows. Using (4.14) and $\Psi^* := \Psi_l(p^k_{n,l} - p^k_{w,l} - p_{c,l}(s^{k,i}_l))$, one obtains

$$\begin{aligned} \left(\tfrac{e^i_{s,l}}{\Delta t},\ e^i_{p_c,l} \right)_{\Omega_l} &= \left(\tfrac{e^i_{s,l}}{\Delta t},\ e^i_{p_c,l} - e^{i-1}_{p_c,l} \right)_{\Omega_l} + \theta \left(\Psi^{k,i}_l - \Psi^* + \Psi^* - \Psi^k_l,\ e^{i-1}_{p_c,l} \right)_{\Omega_l} \\ &\leq \tfrac{1}{\Delta t} \left\| e^i_{s,l} \right\|_{\Omega_l} \left\| e^i_{p_c,l} - e^{i-1}_{p_c,l} \right\|_{\Omega_l} + \theta \left(e^i_{\Psi,l},\ e^{i-1}_{p_c,l} \right)_{\Omega_l} \\ &\quad + \theta \left(\Psi_l \left(p^k_{n,l} - p^k_{w,l} - p_{c,l}(s^{k,i}_l) \right) - \Psi_l \left(p^k_{n,l} - p^k_{w,l} - p_{c,l}(s^k_l) \right),\ e^{i-1}_{p_c,l} \right)_{\Omega_l}. \end{aligned}$$

Since Ψ_l, $p_{c,l}$ are decreasing and Lipschitz-continuous, one gets

$$\left(\tfrac{e^i_{s,l}}{\Delta t},\ e^i_{p_c,l} \right)_{\Omega_l} \leq \tfrac{1}{\Delta t} \left\| e^i_{s,l} \right\|_{\Omega_l} \left\| e^i_{p_c,l} - e^{i-1}_{p_c,l} \right\|_{\Omega_l} - \tfrac{\theta}{L_{\Psi,l}} \left\| e^i_{\Psi,l} \right\|^2_{\Omega_l} + \theta L_{\Psi,l} L_{p_c,l} \left\| e^i_{s_l} \right\|_{\Omega_l} \sum_{\alpha \in \{n,w\}} \left\| e^{i-1}_{p_\alpha,l} \right\|_{\Omega_l}.$$

With the estimate (4.15), Young's inequality yields for $\epsilon_\alpha > 0$

$$\left(\frac{e^i_{s,l}}{\Delta t},\ e^i_{p_c,l}\right)_{\Omega_l} \leq \left(\frac{2\phi_l\theta^2}{\mathcal{L}_{p,l}} + \sum_{\alpha\in\{n,w\}} \frac{\Delta t^2\theta^4 L^2_{\Psi,l}L^2_{p_c,l}}{\epsilon_\alpha} - \frac{\theta}{L_{\Psi,l}}\right)\left\|e^i_{\Psi,l}\right\|^2_{\Omega_l} + \frac{\mathcal{L}_{p,l}}{2\phi_l}\left\|e^i_{p_c,l} - e^{i-1}_{p_c,l}\right\|^2_{\Omega_l} + \sum_{\alpha\in\{n,w\}} \epsilon_\alpha \left\|e^{i-1}_{p_\alpha,l}\right\|^2_{\Omega_l}.$$

The Poincaré inequality (with C_{Ω_l} the domain dependent constant) leads to

$$\left(\frac{e^i_{s,l}}{\Delta t},\ e^i_{p_c,l}\right)_{\Omega_l} \leq \left(\frac{2\phi_l\theta^2}{\mathcal{L}_{p,l}} + \sum_{\alpha\in\{n,w\}} \frac{\Delta t^2\theta^4 L^2_{\Psi,l}L^2_{p_c,l}}{\epsilon_\alpha} - \frac{\theta}{L_{\Psi,l}}\right)\left\|e^i_{\Psi,l}\right\|^2_{\Omega_l} + \frac{\mathcal{L}_{p,l}}{2\phi_l}\left\|e^i_{p_c,l} - e^{i-1}_{p_c,l}\right\|^2_{\Omega_l} + \sum_{\alpha\in\{n,w\}} \frac{\epsilon_\alpha C^2_{\Omega_l}}{\underline{K}_l}\left\|K_l^{1/2}\nabla e^{i-1}_{p_\alpha,l}\right\|^2_{\Omega_l}.$$

Multiplying this estimate by ϕ_l, choosing $\epsilon_\alpha = \theta m_{\lambda_\alpha,l}\underline{K}_l(4\phi_l C^2_{\Omega_l})^{-1}$, and adding to (4.18), one is left with

$$\frac{\mathcal{L}_{p,l}}{2}\left(\left\|e^i_{p_c,l}\right\|^2_{\Omega_l} - \left\|e^{i-1}_{p_c,l}\right\|^2_{\Omega_l}\right) + \sum_{\alpha\in\{n,w\}} \frac{\theta m_{\lambda_\alpha,l}}{2}\left\|K_l^{1/2}\nabla e^i_{p_\alpha,l}\right\|^2_{\Omega_l} + C_l(\Delta t)\left\|e^i_{\Psi,l}\right\|^2_{\Omega_l} \leq \frac{1}{4\mathcal{L}_\Gamma}\sum_{\alpha\in\{n,w\}}\left(\left\|e^i_{g_\alpha,l}\right\|^2_\Gamma - \left\|e^{i+1}_{g_\alpha,3-l}\right\|^2_\Gamma\right) + \sum_{\alpha\in\{n,w\}} \frac{\theta m_{\lambda_\alpha,l}}{4}\left\|K_l^{1/2}\nabla e^{i-1}_{p_\alpha,l}\right\|^2_{\Omega_l},$$

where

$$C_l(\Delta t) = \frac{\phi_l\theta}{L_{\Psi,l}} - \frac{2\phi_l^2\theta^2}{\mathcal{L}_{p,l}} - \Delta t^2\sum_{\alpha\in\{n,w\}}\left(\frac{4\phi_l^2\theta^3 L^2_{\Psi,l}L^2_{p_c,l}C^2_{\Omega_l}}{m_{\lambda_\alpha,l}\underline{K}_l} + \frac{2\theta^3 L^2_{\lambda_\alpha,l}M^2_{p_\alpha,l}}{m_{\lambda_\alpha,l}}\right).$$

By assumption, $\mathcal{L}_{p,l} > 2\phi_l\theta L_{\Psi,l}$ and Δt is small enough, such that $C_l(\Delta t) \geq 0$. Then, summation of the estimates for $l \in \{1,2\}$ and $i = 1,2,\ldots,r$ yields

$$\sum_{i=1}^{r}\sum_{l=1}^{2}\sum_{\alpha\in\{n,w\}} \frac{\theta m_{\lambda_\alpha,l}}{4}\left\|K_l^{1/2}\nabla e^i_{p_\alpha,l}\right\|^2_{\Omega_l} + \sum_{i=1}^{r}\sum_{l=1}^{2} C_l(\Delta t)\left\|e^i_{\Psi,l}\right\|^2_{\Omega_l} \leq \frac{1}{4\mathcal{L}_\Gamma}\sum_{l=1}^{2}\sum_{\alpha\in\{n,w\}}\left\|e^1_{g_\alpha,l}\right\|^2_\Gamma + \sum_{l=1}^{2}\frac{\mathcal{L}_{p,l}}{2}\left\|e^0_{p_c,l}\right\|^2_{\Omega_l} + \sum_{l=1}^{2}\sum_{\alpha\in\{n,w\}}\frac{\theta m_{\lambda_\alpha,l}}{4}\left\|K_l^{1/2}\nabla e^0_{p_\alpha,l}\right\|^2_{\Omega_l}.$$

Since the righthand side is independent of r, we conclude that the series on the left is absolutely convergent. By the Poincaré inequality and estimate (4.15), we conclude $p^{k,i}_{\alpha,l} \to p^k_{\alpha,l}$ in $\mathcal{W}_l$ and $s^{k,i}_l \to s^k_l$ in $L^2(\Omega_l)$. The weak convergence $e^i_{g_\alpha,l} \rightharpoonup 0$ in $L^2(\Gamma)$ can be shown exactly as in Theorem 4.1 by the limit $i \to \infty$ in (4.11) and (4.12). □

5. Numerical experiments

For the numerical validation of the previous theoretical results, we present several numerical studies in two spatial dimensions. We focus on three aspects: the convergence behavior in space and time of the whole method, the convergence behavior of the LDD-schemes within single time steps, and the choice of the parameters. Three examples with manufactured solution are presented, followed by a realistic application.

The theoretical results above are independent of the spatial discretization. For Richards' equation and two-phase flow models with equilibrium capillary pressure as well as dynamic capillarity, the (mixed) finite element method is used in [2–4], the discontinuous Galerkin method in [5,62] and the finite volume method in [6,63–65]. General gradient schemes are considered in [60,66]. Since the pressure equations are elliptic, we choose here a standard finite element method (Q_2) on a uniform, rectangular mesh of width Δx matching at the interface Γ. Note that this choice is in general not possible for the saturation which lies in $L^2(\Omega_l)$. However, in light of (3.5), the regularity of the saturation is inherited from the initial condition up to $s^0_l \in H^1(\Omega_l)$. This restriction of the initial data is used for the following numerical examples to allow the use of Lagrange finite elements. We use the Crank–Nicolson method ($\theta = 1/2$) in time, so that discretization errors of order $\mathcal{O}(\Delta t^2 + \Delta x^2)$ are expected for sufficiently smooth solutions.

Table 1
Convergence study and average number of LDD-iterations per time step of the LDD-scheme I for varying time step size Δt and mesh width Δx in the case with linear coefficients, but no hysteresis.

Δt	Δx	$\|e_p\|_{L^2(0,T;H^1(\Omega))}$	EOC$_p$	$\|e_s\|_{L^2(0,T;H^1(\Omega))}$	EOC$_s$	Avg.-Iter.
0.2	0.2	$5.352 \cdot 10^{-3}$		$5.824 \cdot 10^{-3}$		13
0.1	0.1	$1.394 \cdot 10^{-3}$	1.94	$1.463 \cdot 10^{-3}$	1.993	12.3
0.05	0.05	$3.564 \cdot 10^{-4}$	1.968	$3.670 \cdot 10^{-4}$	1.995	12
0.025	0.025	$9.013 \cdot 10^{-5}$	1.983	$9.192 \cdot 10^{-5}$	1.997	11.5
0.0125	0.0125	$2.273 \cdot 10^{-5}$	1.987	$2.312 \cdot 10^{-5}$	1.991	15.5

At each time step, the LDD-schemes are stopped, when the relative L^2-norm of the difference of subsequent iterative solutions drops below 10^{-8}. To obtain the implicitly given saturation in the LDD-scheme II, the fixed-point iteration discussed in the proof of Lemma 4.2 is used up to a residual of 10^{-12}. For simplicity, we take the same linearization parameters on both subdomains, i.e. $\mathcal{L}_a := \mathcal{L}_{a,1} = \mathcal{L}_{a,2}$ for $a \in \{p, T, \Phi\}$.

The implementation is done in `C++` using the library `deal.II` [67]. All calculations are performed on a Linux octa-core system.

Note that the mobility functions used in the following examples are not bounded away from zero as required by Assumption 1. However, the initial and boundary conditions are chosen in such a way that a degeneracy does not occur since the saturation solutions are bounded away from 0 and 1. The same results are obtained, when the mobility functions are replaced by a regularization $\lambda^{\varepsilon}_{\alpha,l}(s) = \max\{\varepsilon, \lambda_{\alpha,l}(s)\}$ for some small $\varepsilon > 0$.

5.1. Analytic test cases

For the three examples with manufactured solution, one can explicitly compute the errors and thereby the experimental order of convergence (EOC). For simplicity, we assume an isotropic and constant absolute permeability on the whole domain, i.e. $K_1 = K_2 = 1$, and a constant porosity $\phi_1 = \phi_2 = 1$. We set the final time $T = 1$, and decompose the domain $\Omega = (-1,\ 1) \times (0, 1)$ at the interface $\Gamma = \{0\} \times (0, 1)$ into $\Omega_1 = (-1, 0) \times (0, 1)$ and $\Omega_2 = (0, 1) \times (0, 1)$.

Note that for an anisotropic absolute permeability K_l a suitable spatial discretization is necessary to avoid the discretization errors to depend on the ratio between largest and smallest eigenvalues of K_l. Furthermore, the direction of the anisotropy affects the flux across the interface Γ and thus the optimal choice of the parameter $\mathcal{L}_\Gamma$.

5.1.1. Linear coefficient functions without hysteresis

We consider a simple nonlinear problem with linear coefficient functions, but no hysteresis. These functions are therefore chosen

$$\lambda_n(s) = 1 - s, \qquad \lambda_w(s) = s, \qquad p_c(s, \boldsymbol{x}) = 0.2 - s, \qquad \tau \equiv 1, \qquad \gamma \equiv 0.$$

The righthand side terms are selected such that the analytic solution is given by

$$p_n(\boldsymbol{x}, t) = \tfrac{(1-x_1)(1+x_1)^2}{2(1+t)^2}, \qquad p_w(\boldsymbol{x}, t) = \tfrac{(1-x_1)(1+x_1)^2}{2(1+t)}, \qquad s(\boldsymbol{x}, t) = \tfrac{(1-x_1)(1+x_1)^2}{2(1+t)} + 0.2.$$

This corresponds to homogeneous Dirichlet boundary conditions at $x_1 = \pm 1$ and homogeneous Neumann boundary conditions at $x_2 \in \{0, 1\}$. Note that in this special case, the two schemes almost coincide, since they only differ in the inverted capillary pressure equation, which is a linear transformation here, and thus the results are very similar.

First, we study the convergence order of the two methods with respect to the time step size Δt and the mesh width Δx. For the LDD-scheme I, the parameters are $\mathcal{L}_p = 0.5$, $\mathcal{L}_T = 1$ and $\mathcal{L}_\Gamma = 0.375$ ($\mathcal{L}_\Phi = 0$), while for the LDD-scheme II, the parameters are $\mathcal{L}_p = 0.5$ and $\mathcal{L}_\Gamma = 0.375$. Second order convergence of pressure and saturation is observed for both schemes, as clearly shown in Tables 1 and 2 and Fig. 2. This even holds for the saturation in the $L^2(0, T; H^1(\Omega))$ norm, which is not covered by the above theoretical results.

With decreasing time step size Δt, the average iteration number per time step and thus the convergence rate stay almost constant. This result is surprising, since the convergence rate asymptotically deteriorates for both the L-scheme and the domain decomposition method. For L-schemes, the converge rate typically is $\sqrt{C/(C + \Delta t)}$ for some $C > 0$ (see e.g. [2,4]), and for the domain decomposition method with optimal parameter, one obtains

Table 2
Convergence study and average number of LDD-iterations per time step of the LDD-scheme II for varying time step size Δt and mesh width Δx in the case with linear coefficients, but no hysteresis.

Δt	Δx	$\|e_p\|_{L^2(0,T;H^1(\Omega))}$	EOC$_p$	$\|e_s\|_{L^2(0,T;H^1(\Omega))}$	EOC$_s$	Avg.-Iter.
0.2	0.2	$5.352 \cdot 10^{-3}$		$5.824 \cdot 10^{-3}$		13
0.1	0.1	$1.394 \cdot 10^{-3}$	1.94	$1.463 \cdot 10^{-3}$	1.993	12
0.05	0.05	$3.564 \cdot 10^{-4}$	1.968	$3.670 \cdot 10^{-4}$	1.995	12
0.025	0.025	$9.013 \cdot 10^{-5}$	1.983	$9.192 \cdot 10^{-5}$	1.997	11.3
0.0125	0.0125	$2.273 \cdot 10^{-5}$	1.987	$2.312 \cdot 10^{-5}$	1.991	16.2

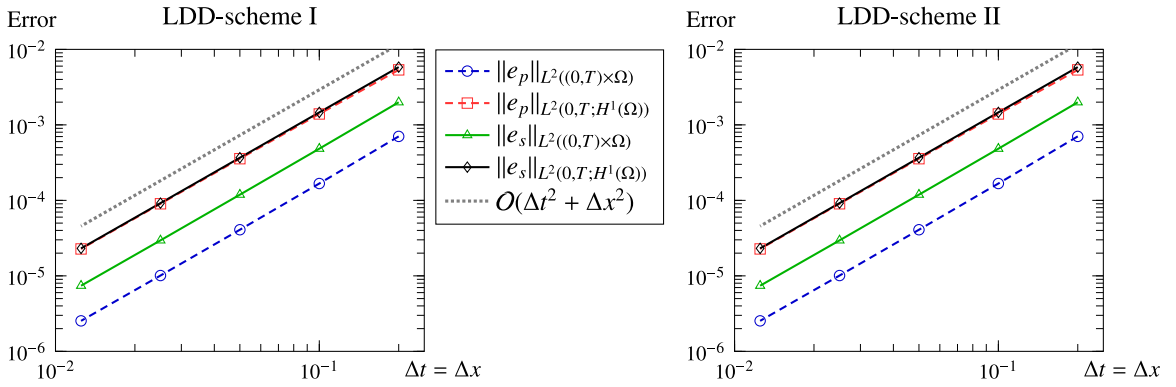

Fig. 2. Second order convergence in time step size Δt and mesh width Δx of pressure and saturation is observed for both LDD-schemes in the case with linear coefficients, but no hysteresis.

convergence rates of $1-\mathcal{O}(\sqrt{\Delta t})$ (see e.g. [14,16]). Here, the pre-asymptotic regime leads to the different behavior, which seems to end around $\Delta t = 0.025$.

Moreover, the analysis provides convergence independently of the initial guess. This can also be observed, when the initial guess in each time step is fixed to $p_n^{k,0} = p_w^{k,0} \equiv 1$ and $s^{k,0} \equiv 0.75$ for the above simulations with $\Delta t = \Delta x = 0.05$. In this case, the resulting errors $\|e_p\|_{L^2(0,T;H^1(\Omega))}$ and $\|e_s\|_{L^2(0,T;H^1(\Omega))}$ are the same as in the studies above ($\pm 0.1\%$), only the average number of LDD-iterations per time step increases by about 20%.

Next, the convergence properties within one time step are considered. Therefore, the relative differences in pressure and saturation between consecutive iterations

$$d_p^i := \sqrt{\left\| \frac{p_n^{k,i} - p_n^{k,i-1}}{p_n^{k,i}} \right\|_{L^2(\Omega)}^2 + \left\| \frac{p_w^{k,i} - p_w^{k,i-1}}{p_w^{k,i}} \right\|_{L^2(\Omega)}^2}, \qquad d_s^i := \left\| \frac{s^{k,i} - s^{k,i-1}}{s^{k,i}} \right\|_{L^2(\Omega)},$$

are plotted in Fig. 3 for the last time step of the above simulations with $\Delta t = \Delta x = 0.05$. These results indicate a very fast, linear convergence. This fast convergence depends on a proper choice of the parameters. To analyze the dependence, we compute the average number of LDD-iterations per time step for several simulations with varying values of $\mathcal{L}_p$, $\mathcal{L}_T$ and $\mathcal{L}_\Gamma$, while $\Delta t = \Delta x = 0.05$ is fixed. The average number of LDD-iterations per time step is minimal for a specific set of parameters and increases drastically for small deviations from that (see Fig. 4). The linearization parameters typically should be chosen as small as possible, but big enough to ensure convergence (see e.g. [2,4,22]). Here, this means that lower bounds from our analysis (see Theorems 4.1 and 4.2) should be good predictions. They are $\mathcal{L}_p \geq 1/2$ and $\mathcal{L}_T \geq 1/2$ for the first scheme and $\mathcal{L}_p > 1$ for the second one, and they are indeed very close to the optimal ones. On the other hand, theoretical prediction of the domain decomposition parameter $\mathcal{L}_\Gamma$ is usually based on the Fourier transformation [14,16,18], which cannot be directly applied to nonlinear problems. Therefore, there are no such predictions available yet for this type of nonlinear equations.

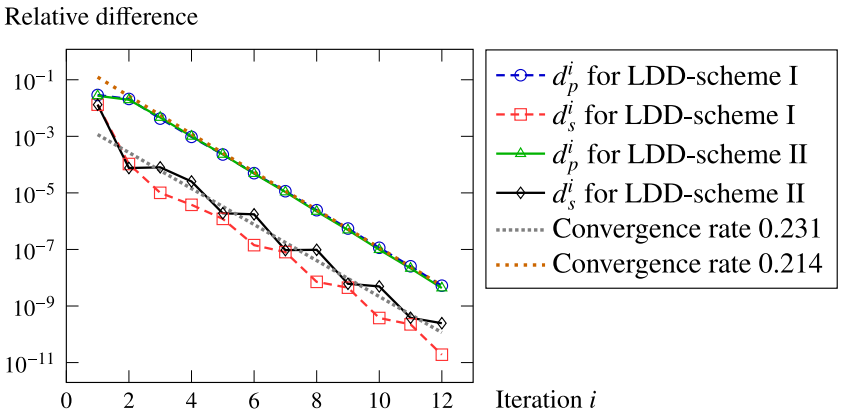

Fig. 3. The LDD-schemes converge very fast and linearly in the last time step of the case with linear coefficient functions, but no hysteresis. Plotted are the relative differences of pressure and saturation between consecutive iterations, together with the fitted convergence rates.

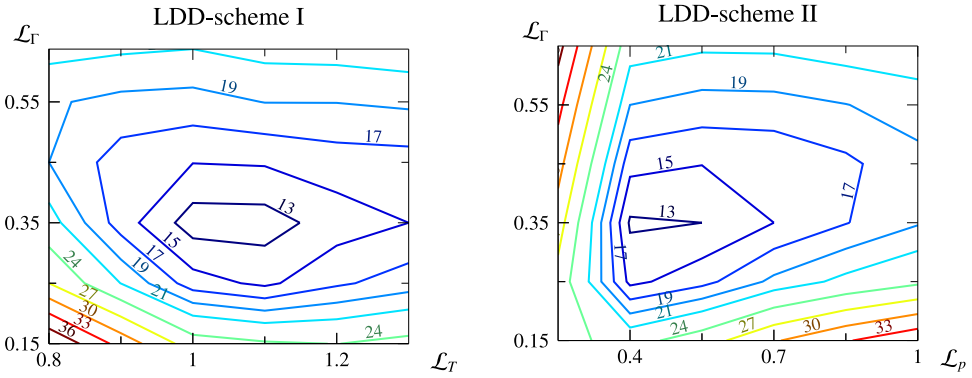

Fig. 4. Parameter dependence of the average number of LDD-iterations per time step for $\Delta t = \Delta x = 0.05$ in the case with linear coefficients, but no hysteresis. For simplicity, $\mathcal{L}_p = 0$ for LDD-scheme I.

5.1.2. *Nonlinear coefficient functions without hysteresis*

Next, we consider a problem with nonlinear coefficient functions, again excluding hysteresis. These functions are

$$\lambda_n(s) = (1-s)^2, \qquad \lambda_w(s) = s^2, \qquad p_c(s, \boldsymbol{x}) = -s^2, \qquad \tau(s) = s, \qquad \gamma \equiv 0.$$

The righthand sides are chosen in such a way that the analytic solution is given by

$$p_n(\boldsymbol{x}, t) = 1 - \frac{(3-2t)(3+2(x_2-x_1))^2}{400}, \qquad p_w(\boldsymbol{x}, t) = 1 + \frac{(3-2t)(3+2(x_2-x_1))^2}{400}, \qquad s(\boldsymbol{x}, t) = \frac{(3+2(x_2-x_1))\sqrt{1+t}}{10},$$

where the corresponding boundary conditions are for simplicity the given exact values, i.e. inhomogeneous Dirichlet values on the whole boundary $\partial\Omega$. Note, that the solutions are polynomials of degree two, and thus the spatial discretization (Q_2) is exact, so that the mesh width $\Delta x = 0.05$ is fixed in the following. The parameters are $\mathcal{L}_p = 0.5$, $\mathcal{L}_T = 0.55$ and $\mathcal{L}_\Gamma = 2.65$ ($\mathcal{L}_\Phi = 0$) for the LDD-scheme I, while $\mathcal{L}_p = 1.5$ and $\mathcal{L}_\Gamma = 2.65$ for the LDD-scheme II.

As before, second order convergence in Δt is achieved by both schemes, again even for the saturation in the $L^2(0, T; H^1(\Omega))$ norm (see Fig. 5 and Tables 3 and 4). The average number of LDD-iterations per time step is two times bigger than in the previous example due to the stronger nonlinearities. This time, it even decreases for decreasing time step size Δt, which indicates here an early pre-asymptotic regime, where the smaller differences between solutions of consecutive time steps lead to a smaller number of necessary iterations. Fixing the initial guess ($s \equiv 0.25$ and $p_n = p_w \equiv 2$) results in the same errors $\|e_p\|_{L^2(0,T;H^1(\Omega))}$ and $\|e_s\|_{L^2(0,T;H^1(\Omega))}$ ($\pm 0.3\%$) as in the

Table 3
Convergence study and average number of LDD-iterations per time step of the LDD-scheme I for varying time step size Δt in the case with nonlinear coefficients, but no hysteresis.

Δt	$\|e_p\|_{L^2(0,T;H^1(\Omega))}$	EOC$_p$	$\|e_s\|_{L^2(0,T;H^1(\Omega))}$	EOC$_s$	Avg.-Iter.
0.2	$1.363 \cdot 10^{-3}$		$3.712 \cdot 10^{-4}$		51.8
0.1	$2.573 \cdot 10^{-4}$	2.405	$8.829 \cdot 10^{-5}$	2.072	46.6
0.05	$6.370 \cdot 10^{-5}$	2.014	$2.174 \cdot 10^{-5}$	2.022	43.2
0.025	$1.584 \cdot 10^{-5}$	2.007	$5.519 \cdot 10^{-6}$	1.978	41.6
0.0125	$4.126 \cdot 10^{-6}$	1.941	$1.665 \cdot 10^{-6}$	1.729	41.1

Table 4
Convergence study and average number of LDD-iterations per time step of the LDD-scheme II for varying time step size Δt in the case with nonlinear coefficients, but no hysteresis.

Δt	$\|e_p\|_{L^2(0,T;H^1(\Omega))}$	EOC$_p$	$\|e_s\|_{L^2(0,T;H^1(\Omega))}$	EOC$_s$	Avg.-Iter.
0.2	$6.017 \cdot 10^{-4}$		$3.036 \cdot 10^{-4}$		49.6
0.1	$1.345 \cdot 10^{-4}$	2.162	$7.200 \cdot 10^{-5}$	2.076	44.5
0.05	$3.181 \cdot 10^{-5}$	2.08	$1.750 \cdot 10^{-5}$	2.04	40.1
0.025	$7.733 \cdot 10^{-6}$	2.04	$4.305 \cdot 10^{-6}$	2.023	36.6
0.0125	$2.020 \cdot 10^{-6}$	1.937	$1.076 \cdot 10^{-6}$	2	33.6

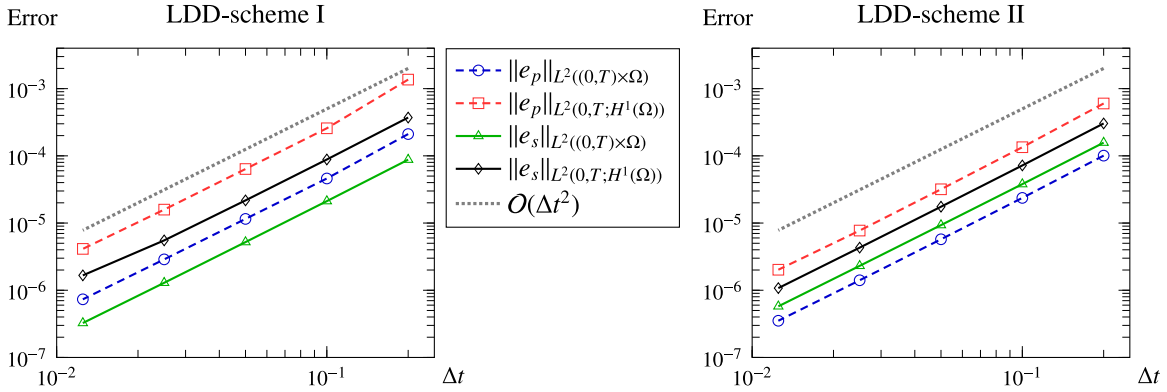

Fig. 5. Second order convergence in the time step size Δt of pressure and saturation is observed for both LDD-schemes in the case with nonlinear coefficients, but no hysteresis.

above studies with $\Delta t = 0.05$, but in a significantly increased number of iterations per time step (71% and 89% for LDD-scheme I and II, respectively).

Next, the convergence properties of the methods within one time step are discussed. In the last time step of the above simulations with $\Delta t = 0.05$, we observe again a fast and almost linear convergence (see Fig. 6). The dependence of the average number of LDD-iterations per time step when varying the LDD-parameters $\mathcal{L}_p$, $\mathcal{L}_T$ and $\mathcal{L}_\Gamma$ is computed for several simulations where $\Delta t = 0.05$ is fixed. As visible Fig. 7, the parameter dependence shows a different behavior in this case. Only the second scheme has an optimal parameter set, whereas the first one shows improving convergence for decreasing $\mathcal{L}_T$, $\mathcal{L}_T \to 0.6$, until it suddenly does not converge any more. The latter agrees very well with the theory, which predicts $\mathcal{L}_p \geq 1$ and $\mathcal{L}_T \geq 1/2$ for the LDD-scheme I, while $\mathcal{L}_p > 1$ for the second one is again very close to the optimum at 1.5. Furthermore, small deviations from the optima have less impact than in the previous example.

5.1.3. Linear coefficient functions including hysteresis

Finally, we consider a problem including hysteresis, where the linear coefficient functions are

$$\lambda_n(s) = 1 - s, \qquad \lambda_w(s) = s, \qquad p_c(s, \boldsymbol{x}) = -s, \qquad \tau \equiv 1, \qquad \gamma \equiv 1.$$

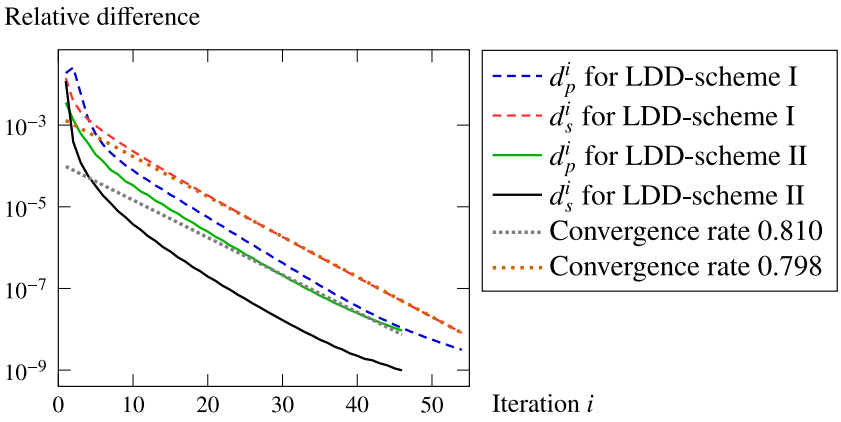

Fig. 6. The LDD-schemes converge fast and almost linearly in the last time step of the case with nonlinear coefficient functions, but no hysteresis. Plotted are the relative differences of pressure and saturation between consecutive iterations, together with the fitted convergence rates.

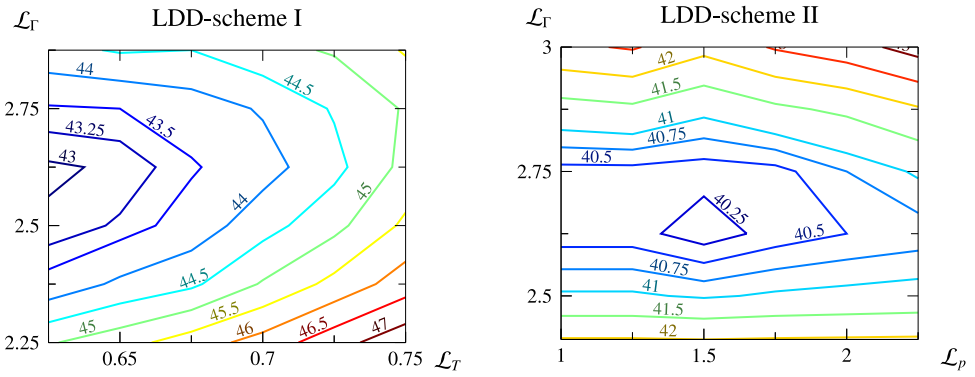

Fig. 7. Parameter dependence of the average number of LDD-iterations per time step for $\Delta t = 0.05$ in the case with nonlinear coefficients, but no hysteresis. For simplicity, $\mathcal{L}_p = 0$ for LDD-scheme I.

Since hysteresis occurs during the change between imbibition and drainage, we construct righthand side terms which yield the following manufactured solution

$$s(\boldsymbol{x},t) = \begin{cases} \frac{1}{2}\cos\left((t_0(\boldsymbol{x})-t)^2\right) & \text{if } t < t_0(\boldsymbol{x}), \\ \frac{1}{2} & \text{if } t_0(\boldsymbol{x}) \le t \le t_1(\boldsymbol{x}), \\ \frac{1}{2}\cos\left((t-t_1(\boldsymbol{x}))^2\right) & \text{if } t_1(\boldsymbol{x}) < t, \end{cases}$$

$$p_n(\boldsymbol{x},t) = \begin{cases} 1-\frac{1}{2}\cos\left((t_0(\boldsymbol{x})-t)^2\right) & \text{if } t < t_0(\boldsymbol{x}), \\ 6\xi^5(t,\boldsymbol{x}) - 15\xi^4(t,\boldsymbol{x}) + 10\xi^3(t,\boldsymbol{x}) + \frac{1}{2} & \text{if } t_0(\boldsymbol{x}) \le t \le t_1(\boldsymbol{x}), \\ 2-\frac{1}{2}\cos((t-t_1(\boldsymbol{x}))^2) & \text{if } t_1(\boldsymbol{x}) < t, \end{cases}$$

$$p_w(\boldsymbol{x},t) = \begin{cases} 2+\sqrt{(t_0(\boldsymbol{x})-t)^2}\sin\left((t_0(\boldsymbol{x})-t)^2\right) & \text{if } t < t_0(\boldsymbol{x}), \\ -6\xi^5(t,\boldsymbol{x}) + 15\xi^4(t,\boldsymbol{x}) - 10\xi^3(t,\boldsymbol{x}) + 2 & \text{if } t_0(\boldsymbol{x}) \le t \le t_1(\boldsymbol{x}), \\ 1-\sqrt{(t-t_1(\boldsymbol{x}))^2}\sin((t-t_1(\boldsymbol{x}))^2) & \text{if } t_1(\boldsymbol{x}) < t, \end{cases}$$

where

$$t_0(\boldsymbol{x}) := \tfrac{10x_1+7}{20}, \qquad t_1(\boldsymbol{x}) := t_0(\boldsymbol{x}) + \tfrac{3}{10} = \tfrac{10x_1+13}{20}, \qquad \xi(t,\boldsymbol{x}) := \tfrac{t-t_0(\boldsymbol{x})}{t_1(\boldsymbol{x})-t_0(\boldsymbol{x})}.$$

The corresponding boundary conditions are simply chosen to be of inhomogeneous Dirichlet type at $x_1 = \pm 1$, and of homogeneous Neumann type at $x_2 \in \{0, 1\}$. For the LDD-scheme I, the regularization parameter is chosen

Table 5
Convergence study and average number of LDD-iterations per time step of the LDD-scheme I for varying time step in the full analytical case with linear coefficients including hysteresis.

Δt	Δx	$\|e_p\|_{L^2(0,T;H^1(\Omega))}$	EOC$_p$	$\|e_s\|_{L^2(0,T;H^1(\Omega))}$	EOC$_s$	Avg.-Iter.
0.5	0.25	0.161		$7.739 \cdot 10^{-2}$		5525
0.2	0.1	$4.600 \cdot 10^{-2}$	1.364	$6.891 \cdot 10^{-3}$	2.64	4890
0.1	0.05	$1.196 \cdot 10^{-2}$	1.943	$1.688 \cdot 10^{-3}$	2.029	4380
0.05	0.025	$3.215 \cdot 10^{-3}$	1.895	$2.336 \cdot 10^{-3}$	−0.469	3900

Table 6
Convergence study and average number of LDD-iterations per time step of the LDD-scheme II for varying time step in the full analytical case with linear coefficients including hysteresis.

Δt	Δx	$\|e_p\|_{L^2(0,T;H^1(\Omega))}$	EOC$_p$	$\|e_s\|_{L^2(0,T;H^1(\Omega))}$	EOC$_s$	Avg.-Iter.
0.2	0.05	$1.534 \cdot 10^{-2}$		$5.631 \cdot 10^{-3}$		17.8
0.1	0.025	$3.788 \cdot 10^{-3}$	2.018	$1.309 \cdot 10^{-3}$	2.105	17
0.05	0.0125	$9.454 \cdot 10^{-4}$	2.002	$3.147 \cdot 10^{-4}$	2.056	16.5
0.025	0.0063	$2.345 \cdot 10^{-4}$	2.011	$7.640 \cdot 10^{-5}$	2.042	15.6

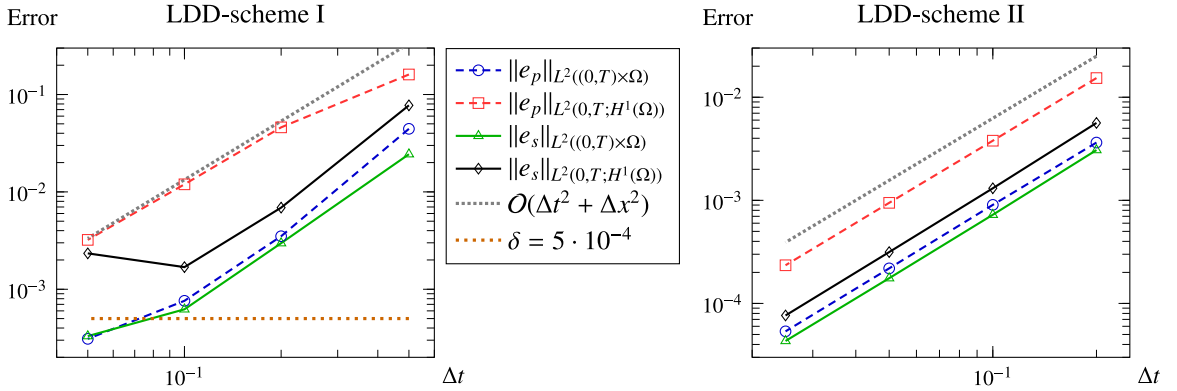

Fig. 8. Second order convergence in time step size Δt and mesh width Δx of pressure and saturation is observed for both LDD-schemes in the case with linear coefficients, including hysteresis. The accuracy of the first scheme is limited by the regularization (parameter δ), as visible for e.g. the saturation. The mesh width is $\Delta x = \Delta t/2$ for LDD-scheme I and $\Delta x = \Delta t/4$ for LDD-scheme II.

$\delta = 5 \cdot 10^{-4}$ and the LDD-parameters are $\mathcal{L}_p = 0.5$, $\mathcal{L}_T = 2$, $\mathcal{L}_\Phi = 10^3$ and $\mathcal{L}_\Gamma = 0.375$. In this case, we use a reduced stopping criterion for the LDD-scheme of 10^{-7}. For the LDD-scheme II, the parameters are $\mathcal{L}_p = 0.33$ and $\mathcal{L}_\Gamma = 0.375$.

As before, second order convergence with respect to the time step size Δt and mesh width Δx is observed for both schemes, until the errors due to regularization are dominating in the first scheme (see Tables 5 and 6 and Fig. 8). Here, the inverted formulation of the second scheme is clearly advantageous. While the first scheme needs a huge parameter $\mathcal{L}_\Phi$ for a moderate regularization parameter δ due to the steep slope in the capillary pressure equation near zero, the second scheme has no such restriction due to the inverted formulation. Therefore, the average number of iterations per time step for the LDD-scheme I is huge, which makes this scheme unpractical for such problems. In contrast, the average number of iteration for the LDD-scheme II is much lower, which again shows that the latter is the preferable method for this type of applications. As before, we observe the iteration number to decrease for decreasing time step size due to the pre-asymptotic regime. Furthermore, if the initial guess is fixed to $s^{k,0} \equiv 0.75$ and $p_n^{k,0} = p_w^{k,0} \equiv 1$ in each time step, the errors are similar to those in the original studies with $\Delta t = 0.1$, (+35% for LDD-scheme I, ±0.1% for LDD-scheme II).

The convergence is almost linear for both schemes, but only the LDD-scheme II is fast (see Fig. 9). The first scheme has a convergence rate of 0.999 and thus should not be used for applications including hysteresis, or at least needs to be improved by e.g. localizing the LDD-parameter. Nevertheless, it has good convergence properties within the first few iterations, and hence could be used as a preconditioner. The dependence of the average number of

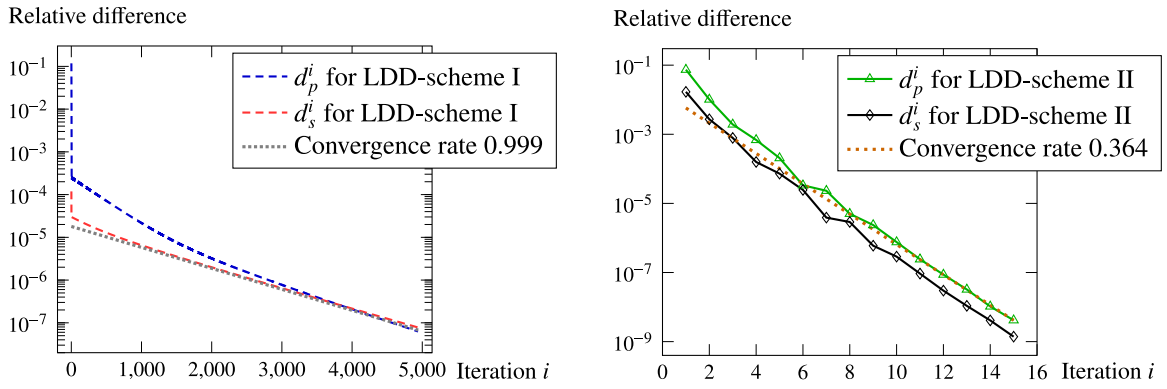

Fig. 9. Both LDD-schemes converge almost linearly, but only the second one is fast in the last time step of the case with linear coefficient functions including hysteresis, for $\Delta t = 0.05$ and $\Delta x = 0.025$ (left) or $\Delta x = 0.0125$ (right). Plotted are the relative differences of pressure and saturation between consecutive iterations, together with the fitted convergence rates.

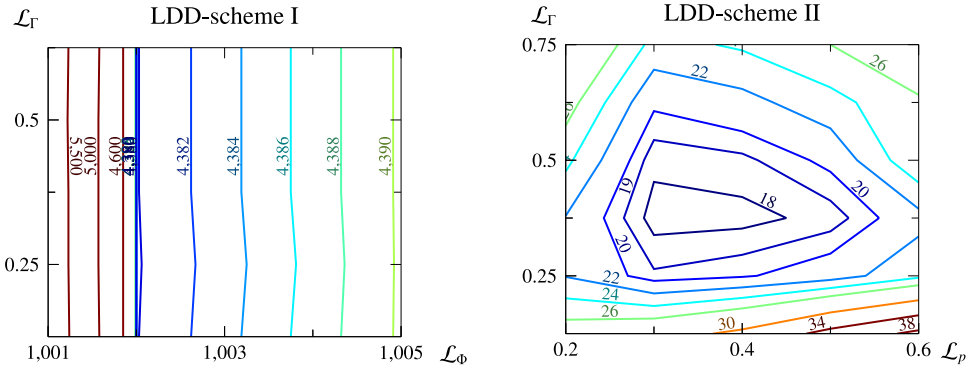

Fig. 10. Parameter dependence of the average number of iterations per time step in the analytical case with linear coefficients including hysteresis. *Left:* $\delta = 5 \cdot 10^{-4}$, $\Delta t = 0.1$, $\Delta x = 0.05$. For simplicity $\mathcal{L}_p = \mathcal{L}_T = 0$. *Right:* $\Delta t = 0.1$, $\Delta x = 0.025$.

iterations per time step on the LDD-parameters $\mathcal{L}_\Phi$, $\mathcal{L}_p$ and $\mathcal{L}_\Gamma$ based on several simulations with fixed discretization is similar to the previous example. Only the LDD-scheme II has a clear optimal parameter set, whereas the first one shows almost no dependence on the domain decomposition parameter $\mathcal{L}_\Gamma$ (see Fig. 10). The lower bounds from our analysis are in this case $\mathcal{L}_p \geq 1/2$, $\mathcal{L}_T \geq 1/2$ and $\mathcal{L}_\Phi \geq 10^3$ for LDD-scheme I and $\mathcal{L}_p > 1$ for the second one. For the first scheme, this coincides very well with the observed optimum, while the bound for the second one is too restrictive for this application, but a good indicator of the optimal region.

5.2. Realistic test case

This last subsection is dedicated to the study of a realistic problem including gravity. To this end, we choose a van-Genuchten–Mualem parameterization [68], with the relative permeabilities and the equilibrium capillary pressure given by

$$k_n(s) := \sqrt{1 - s_{\text{eff}}}\left(1 - s_{\text{eff}}^{1/m}\right)^{2m}, \qquad k_w(s) := \sqrt{s_{\text{eff}}}\left(1 - \left(1 - s_{\text{eff}}^{1/m}\right)^{m}\right)^{2},$$

$$\tilde{p}_c(s, \boldsymbol{x}) := P\left(s_{\text{eff}}^{-1/m} - 1\right)^{1-m} - (\rho_n - \rho_w) g x_1, \qquad s_{\text{eff}} := \frac{s - s_{\text{wr}}}{1 - s_{\text{wr}} - s_{\text{nr}}},$$

where the effective saturation s_{eff} accounts for the residual saturations s_{nr} and s_{wr}. The capillary pressure is scaled by a material-specific pressure P, and the retention exponent $m > 0$ determines the steepness of the S-shaped curve. Note that this choice of $\tilde{p}_c$ limits the possible range of s to $(s_{\text{wr}}, 1 - s_{\text{nr}}]$. Since $\tilde{p}_c(s, \boldsymbol{x}) \to -(\rho_n - \rho_w) g x_1$ as $s \to 1 - s_{\text{nr}}$, while $\tilde{p}_c(s, \boldsymbol{x}) \to \infty$ as $s \to s_{\text{wr}}$ independently of the chosen parameters P and m, this excludes

Table 7
Parameters of the van-Genuchten–Mualem model in the two subdomains for the realistic case.

Parameter	Symbol	Value		Unit
		Ω_1	Ω_2	
Porosity	ϕ	0.4	0.3	m^2
Absolute permeability	$\tilde{K}$	$3.0 \cdot 10^{-10}$	$5.0 \cdot 10^{-10}$	m^2
Material-specific pressure	P	$1.25 \cdot 10^3$	$1.0 \cdot 10^3$	Pa
Retention exponent	m	0.8	0.7	–
Residual saturation, non-wetting phase	s_{nr}	0.1	0.05	–
Residual saturation, wetting phase	s_{wr}	0.1	0.05	–
Typical redistribution parameter	$\tilde{\tau}$	$2.0 \cdot 10^3$	$1.5 \cdot 10^3$	Pa s
Hysteresis pressure parameter	$\tilde{\gamma}$	200	100	Pa
Density of the non-wetting phase	ρ_n	1.0		kg/m^3
Density of the wetting phase	ρ_w	$1.0 \cdot 10^3$		kg/m^3
Gravity (positive x-direction)	g	9.81		m/s^2
Viscosity of the non-wetting phase	μ_n	$2.0 \cdot 10^{-5}$		Pa s
Viscosity of the wetting phase	μ_w	$1.0 \cdot 10^{-3}$		Pa s

the occurrence of entry-pressures as discussed in Remark 2.1. Furthermore, we include dynamic capillarity and hysteresis by constant τ and γ within each subdomain. All the parameters are listed in Table 7 and inspired by the choices made in [69].

To obtain the non-dimensional equations (2.1)–(2.6), we choose the scaling parameters $L = 1$ m, $p^* = 2.5 \cdot 10^3$ Pa and $\tau^* = 1.5 \cdot 10^3$ Pa s and

$$\lambda_\alpha(s) = \frac{\tau^*}{\mu_\alpha} k_\alpha(s), \qquad K = \frac{\tilde{K}}{L^2}, \qquad p_c(s) = \frac{\tilde{p}_c(s)}{p^*}, \qquad \tau = \frac{\tilde{\tau}}{\tau^*}, \qquad \gamma = \frac{\tilde{\gamma}}{p^*}.$$

The domain $\Omega = (-0.5,\ 0.5) \times (0, 1)$ is decomposed into two subdomains at the interface $\Gamma = \{0\} \times (0, 1)$. We choose the final time $T = 400$ (real time 240 s) and initial conditions with almost constant saturation given by

$$p_n^0(\boldsymbol{x}) = 0.75 - \frac{\rho_n g L}{p^*} x_1 = 0.75 - 0.003924 x_1, \qquad p_w^0(\boldsymbol{x}) = -\frac{\rho_w g L}{p^*} x_1 = -3.924 x_1,$$

$$s^0(\boldsymbol{x}) = p_c^{-1}\left(p_n^0(\boldsymbol{x}) - p_w^0(\boldsymbol{x})\right) \approx \begin{cases} 0.2431 & \text{if } x_1 < 0, \\ 0.2414 & \text{if } x_1 > 0. \end{cases}$$

The boundary conditions at $x_1 = \pm 0.5$ are of constant Dirichlet type, to match the initial conditions, except for p_w at $x_1 = -0.5$ given by

$$p_w\big|_{x_1=-0.5} = 1.962 + \begin{cases} 0.015t & \text{if } t < 25, \\ 0.375 & \text{if } 25 \le t < 100, \\ 0.015(125 - t) & \text{if } 100 \le t < 130, \\ -0.075 & \text{if } 125 \le t, \end{cases}$$

whereas the boundary conditions at $x_2 \in \{0, 1\}$ are of homogeneous Neumann type. By this choice, we simulate an imbibition and drainage cycle. The order of the spatial discretization is reduced to one, i.e. piece-wise linear, and the tolerance for the LDD-schemes is 10^{-6}, since the solution is less smooth than in the analytical cases. In contrast to the manufactured examples above, we only study the convergence of the LDD-schemes within the time steps. Therefore, the mesh width $\Delta x = 0.02$ and $\Delta t = 0.1$ are fixed. Note that the time step size here is about 100 times larger than in [69]. This might partially be a consequence of the different parameters and scaling, but also due to the L-scheme, whereas the Newton method is used in [69].

The choice of the parameters and the results are shown in Table 8, and the obtained solutions for $\mathcal{L}_\Gamma = 0.25$ at time $t \in \{100, 200, 400\}$ are depicted in Fig. 11. The solutions of both methods are very similar and the imbibition and drainage cycle can be clearly observed. The small small peaks near $x_1 = 0$ probably result from the hysteresis. Due to the higher permeability in the second domain, the latter imbibes the wetting phase from the first domain, such that the region in the first domain close to the interface is rather draining. Together with the different equilibrium capillary pressure, this leads to a saturation discontinuity at the interface. Note that the $L^2((0, T) \times \Gamma)$-norm of the flux jumps due to the domain decomposition is below 10^{-3}, and thus smaller than the expected discretization

Table 8
Average number of iterations per time step and $L^2((0,T)\times\Gamma)$-norm of the jump in pressures and of the jump in the fluxes for the realistic problem for varying time step Δt and mesh width Δx with two parameters $\mathcal{L}_\Gamma = 0.25$ (top) and $\mathcal{L}_\Gamma = 0.01$ (bottom). The other parameters of the LDD-scheme I are $\mathcal{L}_p = 1.0$, $\mathcal{L}_T = 1.3$, $\mathcal{L}_\Phi = 40$ and $\delta = 10^{-3}$. The other parameter of the second scheme is $\mathcal{L}_p = 2.0$.

$\mathcal{L}_\Gamma = 0.25$	dt	dx	Avg.-Iter.	$\|[p_\alpha]\|_{L^2((0,T)\times\Gamma)}$	$\|[\boldsymbol{u}_\alpha \cdot \boldsymbol{\nu}]\|_{L^2((0,T)\times\Gamma)}$
LDD-scheme I	0.5	0.1	1480.3	$6.22 \cdot 10^{-5}$	$1.68 \cdot 10^{-3}$
	0.2	0.05	954.8	$8.29 \cdot 10^{-5}$	$1.32 \cdot 10^{-3}$
	0.1	0.02	626.5	$1.13 \cdot 10^{-4}$	$9.89 \cdot 10^{-4}$
LDD-scheme II	0.5	0.1	410.8	$9.77 \cdot 10^{-6}$	$1.61 \cdot 10^{-3}$
	0.2	0.05	212.7	$1.65 \cdot 10^{-5}$	$1.06 \cdot 10^{-3}$
	0.1	0.02	69.9	$3.65 \cdot 10^{-5}$	$4.42 \cdot 10^{-4}$
$\mathcal{L}_\Gamma = 0.01$	dt	dx	Avg.-Iter.	$\|[p_\alpha]\|_{L^2((0,T)\times\Gamma)}$	$\|[\boldsymbol{u}_\alpha \cdot \boldsymbol{\nu}]\|_{L^2((0,T)\times\Gamma)}$
LDD-scheme I	0.5	0.1	147.4	$5.31 \cdot 10^{-5}$	$1.67 \cdot 10^{-3}$
	0.2	0.05	134.4	$5.76 \cdot 10^{-5}$	$1.33 \cdot 10^{-3}$
	0.1	0.02	128.5	$8.60 \cdot 10^{-5}$	$1.00 \cdot 10^{-3}$
LDD-scheme II	0.5	0.1	393.4	$1.72 \cdot 10^{-5}$	$1.65 \cdot 10^{-3}$
	0.2	0.05	209.8	$2.21 \cdot 10^{-5}$	$1.21 \cdot 10^{-3}$
	0.1	0.02	77.7	$1.54 \cdot 10^{-5}$	$1.05 \cdot 10^{-3}$

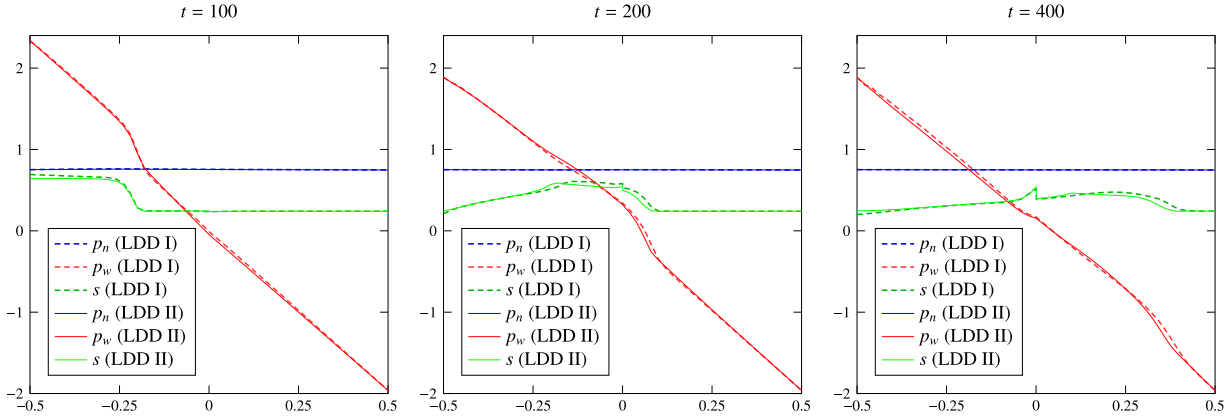

Fig. 11. Numerical solution for the realistic case over x_1, at $x_2 = 0.5$ and the times $t = 100$ (left), $t = 200$ (center) and $t = 400$ (right). Dashed: LDD-scheme I. Solid: LDD-scheme II.

errors. Furthermore, they decrease when the time step size and the mesh width are reduced, although at a sub-linear rate (see Table 8). The norms of the jump in the pressures remain one magnitude lower. Hence, the possibility of numerical artifacts cannot be excluded with certainty. Again, the huge parameter $\mathcal{L}_\Phi$ slows down the LDD-scheme I, whereas the second scheme has no such restriction. Although the average number of iterations per time step for the LDD-scheme I is much smaller than in the last example, the average number of iterations per time step for the LDD-scheme II is up to eight times smaller for small time step sizes. Note that both schemes are used with smaller linearization parameters than those required by our analysis in Section 4, but give rise to better results than the required ones.

This time, we consider the convergence properties of the methods within one time step at the times $t = 150$ and $t = 250$. The first is shortly before the flow passes Γ, while the process switches at Γ from imbibition to drainage around the latter time. For both schemes, we observe convergence rates close to one (see Fig. 12), such that both schemes are slow and should be improved by e.g. localized linearization parameters. Nevertheless, the convergence is almost monotonous, and the differences again decrease rapidly at the beginning. Since such problems would require different parameters for the two subdomains, which makes a proper choice even more challenging, here we

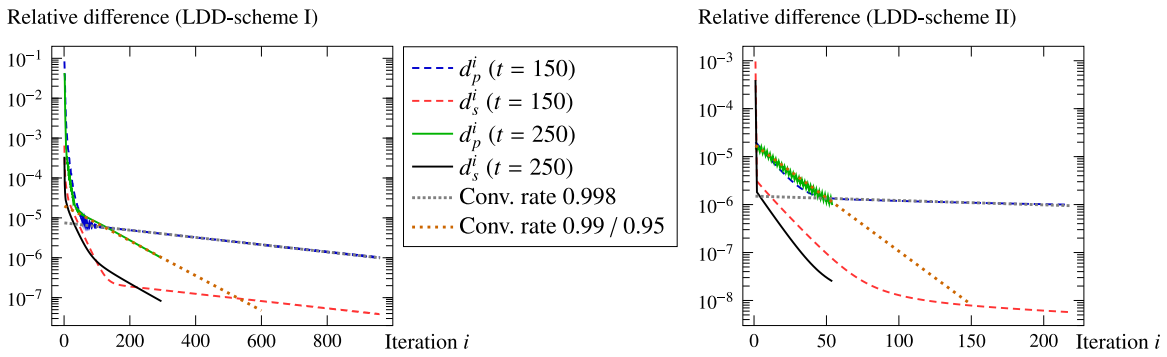

Fig. 12. Both LDD-schemes converge very slowly and rather monotonous, at times $t = 150$ and $t = 250$ of the realistic case for $\Delta t = 0.1$ and $\Delta x = 0.02$ with $\mathcal{L}_\Gamma = 0.25$. Plotted are the relative differences of pressure and saturation between consecutive iterations, together with the fitted convergence rates.

do not study the effect of varying parameters. However, note that the choice of $\mathcal{L}_\Gamma$ strongly affects the efficiency of the first LDD-scheme, while the second one seems rather robust.

6. Conclusion

Linearization and domain decomposition can be combined into one iteration, the LDD-scheme. For the considered non-equilibrium two-phase model, the proposed LDD-schemes lead to unique solutions, which converge towards the semi-discrete solutions of the model, as proven in Section 4. This convergence is global, i.e. independent of the initial guess, and requires only a mild restriction on the time step, independent of the spatial discretization. The inverted formulation for the capillary pressure in the LDD-scheme II avoids the necessary regularization for the original formulation in the LDD-scheme I.

The stability and robustness of both LDD-schemes were numerically verified for several spatially two-dimensional cases. The convergence rate can be improved significantly by a proper choice of the LDD-parameters. In particular, we pointed out the practical advantages of the second scheme, when hysteresis is present. While the analysis leads to good estimates for the linearization parameters, an estimate for the domain decomposition parameter is still an open problem.

The methods can be generalized, when the porosity ϕ and the dynamic capillarity coefficient τ are spatially variable, and when the hysteresis coefficient γ depends on the saturation s. Furthermore, the required regularity of the parameter functions may be relaxed to Hölder continuity as in [7,8]. The degenerated cases $\lambda_w(0) = 0$ and $\lambda_n(1) = 0$ involve difficulties which need to be investigated in future, as well as vanishing dynamic capillarity $\tau = 0$. Nonlinear interface conditions for entry-pressure models can be studied as soon as extensions for the case of dynamic and hysteretic capillarity are available.

The convergence properties of the schemes can be further improved by choosing the LDD-parameters depending on the position or the current solution. Finally, an a-posteriori error analysis can lead to estimates for efficient and adaptive stopping criteria, which would increase the performance even more.

Declaration of competing interest

The authors declare that they have no known competing financial interests or personal relationships that could have appeared to influence the work reported in this paper.

Acknowledgments

This work was supported by the Hasselt University (Project BOF17NI01) and the Research Foundation Flanders (FWO, Project G051418N). We also would like to thank the anonymous referees for their careful reading and constructive suggestions to improve the paper.

References

[1] F.A. Radu, I.S. Pop, P. Knabner, Newton-type methods for the mixed finite element discretization of some degenerate parabolic equations, in: Numerical Mathematics and Advanced Applications ENUMATH 2005, Springer Berlin Heidelberg, 2006, pp. 1192–1200.

[2] I.S. Pop, F.A. Radu, P. Knabner, Mixed finite elements for the Richards' equation: Linearization procedure, J. Comput. Appl. Math. 168 (2004) 365–373.

[3] X. Cao, K. Mitra, Error estimates for a mixed finite element discretization of a two-phase porous media flow model with dynamic capillarity, J. Comput. Appl. Math. 353 (2019) 164–178.

[4] F. List, F.A. Radu, A study on iterative methods for solving Richards' equation, Comput. Geosci. 20 (2016) 341–353.

[5] S. Karpinski, I.S. Pop, F.A. Radu, Analysis of a linearization scheme for an interior penalty discontinuous Galerkin method for two-phase flow in porous media with dynamic capillarity effects, Internat. J. Numer. Methods Engrg. 112 (2017) 553–577.

[6] X. Cao, S.F. Nemadjieu, I.S. Pop, Convergence of an MPFA finite volume scheme for a two-phase porous media flow model with dynamic capillarity, IMA J. Numer. Anal. 39 (2018) 512–544.

[7] F.A. Radu, K. Kumar, J.M. Nordbotten, I.S. Pop, A robust, mass conservative scheme for two-phase flow in porous media including Hölder continuous nonlinearities, IMA J. Numer. Anal. 38 (2017) 884–920.

[8] J.W. Both, K. Kumar, J.M. Nordbotten, I.S. Pop, F.A. Radu, Iterative linearization schemes for doubly degenerate parabolic equations, in: Numerical Mathematics and Advanced Applications ENUMATH 2017, Springer International Publishing, 2019, pp. 49–63.

[9] H.A. Schwarz, Über einen Grenzübergang durch alternierendes Verfahren, Vierteljahrsschr. Naturforschenden Gesellschaft Zür. 15 (1870) 272–286.

[10] P.-L. Lions, On the Schwarz alternating method. I, in: First International Symposium on Domain Decomposition Methods for Partial Differential Equations, 1988, pp. 1–42.

[11] P.-L. Lions, On the Schwarz alternating method III: A variant for nonoverlapping subdomains, in: Third International Symposium on Domain Decomposition Methods for Partial Differential Equations, SIAM, 1990, pp. 202–223.

[12] M.J. Gander, L. Halpern, F. Nataf, Optimal Schwarz waveform relaxation for the one dimensional wave equation, SIAM J. Numer. Anal. 41 (2003) 1643–1681.

[13] M.J. Gander, C. Rohde, Overlapping Schwarz waveform relaxation for convection-dominated nonlinear conservation laws, SIAM J. Sci. Comput. 27 (2005) 415–439.

[14] M.J. Gander, L. Halpern, Optimized Schwarz waveform relaxation methods for advection reaction diffusion problems, SIAM J. Numer. Anal. 45 (2007) 666–697.

[15] F. Caetano, M.J. Gander, L. Halpern, J. Szeftel, Schwarz waveform relaxation algorithms for semilinear reaction-diffusion equations, Netw. Heterog. Media 5 (2010) 487–505.

[16] M.J. Gander, O. Dubois, Optimized Schwarz methods for a diffusion problem with discontinuous coefficient, Numer. Algorithms 69 (2015) 109–144.

[17] M.J. Gander, S.B. Lunowa, C. Rohde, Non-overlapping Schwarz waveform-relaxation for quasi-linear convection-diffusion equations, 2020, In preparation.

[18] D.-G. Calugaru, D. Tromeur-Dervout, Non-overlapping DDMs to solve flow in heterogeneous porous media, in: Domain Decomposition Methods in Science and Engineering, Springer-Verlag, 2005, pp. 529–536.

[19] H. Berninger, R. Kornhuber, O. Sander, Convergence behaviour of Dirichlet–Neumann and Robin methods for a nonlinear transmission problem, in: Domain Decomposition Methods in Science and Engineering XIX, Springer, 2011, pp. 87–98.

[20] E. Ahmed, S.A. Hassan, C. Japhet, M. Kern, M. Vohralí k, A posteriori error estimates and stopping criteria for space-time domain decomposition for two-phase flow between different rock types, SMAI J. Comput. Math. 5 (2019) 195–227.

[21] E. Ahmed, Splitting-based domain decomposition methods for two-phase flow with different rock types, Adv. Water Resour. 134 (2019) 103431.

[22] D. Seus, K. Mitra, I.S. Pop, F.A. Radu, C. Rohde, A linear domain decomposition method for partially saturated flow in porous media, Comput. Methods Appl. Mech. Engrg. 333 (2018) 331–355.

[23] D. Seus, F.A. Radu, C. Rohde, A linear domain decomposition method for two-phase flow in porous media, in: Numerical Mathematics and Advanced Applications ENUMATH 2017, Springer International Publishing, 2019, pp. 603–614.

[24] E. Ahmed, A. Fumagalli, A. Budiša, E. Keilegavlen, J.M. Nordbotten, F.A. Radu, Robust linear domain decomposition schemes for reduced non-linear fracture flow models, 2019, arXiv:1906.05831.

[25] S.B. Lunowa, Linearization and Domain Decomposition Methods for Two-Phase Flow in Porous Media (Master's thesis), Eindhoven University of Technology, 2018, https://research.tue.nl/en/studentTheses/linearization-and-domain-decomposition-methods.

[26] S.B. Lunowa, I.S. Pop, B. Koren, A linear domain decomposition method for non-equilibrium two-phase flow models, in: Numerical Mathematics and Advanced Applications ENUMATH 2019, Springer, 2020, accepted. Preprint available at https://www.uhasselt.be/Documents/CMAT/Preprints/2019/UP1914.pdf.

[27] C.J. van Duijn, J. Molenaar, M.J. de Neef, The effect of capillary forces on immiscible two-phase flow in heterogeneous porous media, Transp. Porous Media 21 (1995) 71–93.

[28] F. Buzzi, M. Lenzinger, B. Schweizer, Interface conditions for degenerate two-phase flow equations in one space dimension, Analysis 29 (2009) 299–316.

[29] C. Cancès, M. Pierre, An existence result for multidimensional immiscible two-phase flows with discontinuous capillary pressure field, SIAM J. Math. Anal. 44 (2012) 966–992.

[30] C.J. van Duijn, X. Cao, I.S. Pop, Two-phase flow in porous media: Dynamic capillarity and heterogeneous media, Transp. Porous Media 114 (2016) 283–308.

[31] D.A. DiCarlo, Experimental measurements of saturation overshoot on infiltration, Water Resour. Res. 40 (2004) W04215.

[32] S. Bottero, S.M. Hassanizadeh, P.J. Kleingeld, T.J. Heimovaara, Nonequilibrium capillarity effects in two-phase flow through porous media at different scales, Water Resour. Res. 47 (2011) W10505.
[33] L. Zhuang, S.M. Hassanizadeh, C.-Z. Qin, A. de Waal, Experimental investigation of hysteretic dynamic capillarity effect in unsaturated flow, Water Resour. Res. 53 (2017) 9078–9088.
[34] L. Zhuang, S.M. Hassanizadeh, C.J. van Duijn, S. Zimmermann, I. Zizina, R. Helmig, Experimental and numerical studies of saturation overshoot during infiltration into a dry soil, Vadose Zone J. 18 (2019) 180167.
[35] J.C. Parker, R.J. Lenhard, A model for hysteretic constitutive relations governing multiphase flow: 1. Saturation-pressure relations, Water Resour. Res. 23 (1987) 2187–2196.
[36] R. Helmig, A. Weiss, B.I. Wohlmuth, Dynamic capillary effects in heterogeneous porous media, Comput. Geosci. 11 (2007) 261–274.
[37] J. Niessner, S.M. Hassanizadeh, A model for two-phase flow in porous media including fluid-fluid interfacial area, Water Resour. Res. 44 (2008).
[38] R. Helmig, A. Weiss, B.I. Wohlmuth, Variational inequalities for modeling flow in heterogeneous porous media with entry pressure, Comput. Geosci. 13 (2009) 373–389.
[39] I.S. Pop, C.J. van Duijn, J. Niessner, S.M. Hassanizadeh, Horizontal redistribution of fluids in a porous medium: The role of interfacial area in modeling hysteresis, Adv. Water Resour. 32 (2009) 383–390.
[40] A. Papafotiou, H. Sheta, R. Helmig, Numerical modeling of two-phase hysteresis combined with an interface condition for heterogeneous porous media, Comput. Geosci. 14 (2009) 273–287.
[41] C.J. van Duijn, K. Mitra, Hysteresis and horizontal redistribution in porous media, Transp. Porous Media 122 (2018) 375–399.
[42] S.M. Hassanizadeh, W.G. Gray, Thermodynamic basis of capillary pressure in porous media, Water Resour. Res. 29 (1993) 3389–3405.
[43] A.Y. Beliaev, S.M. Hassanizadeh, A theoretical model of hysteresis and dynamic effects in the capillary relation for two-phase flow in porous media, Transp. Porous Media 43 (2001) 487–510.
[44] B. Schweizer, Instability of gravity wetting fronts for Richards equations with hysteresis, Interfaces Free Bound. 14 (2012) 37–64.
[45] R. Hilfer, R. Steinle, Saturation overshoot and hysteresis for twophase flow in porous media, Eur. Phys. J. Spec. Top. 223 (2014) 2323–2338.
[46] A. Rätz, B. Schweizer, Hysteresis models and gravity fingering in porous media, Z. Angew. Math. Mech. 94 (2014) 645–654.
[47] K. Mitra, C.J. van Duijn, Wetting fronts in unsaturated porous media: The combined case of hysteresis and dynamic capillary pressure, Nonlinear Anal. RWA 50 (2019) 316–341.
[48] B. Schweizer, The Richards equation with hysteresis and degenerate capillary pressure, J. Differential Equations 252 (2012) 5594–5612.
[49] J. Koch, A. Rätz, B. Schweizer, Two-phase flow equations with a dynamic capillary pressure, Eur. J. Appl. Math. 24 (2012) 49–75.
[50] X. Cao, I.S. Pop, Two-phase porous media flows with dynamic capillary effects and hysteresis: Uniqueness of weak solutions, Comput. Math. Appl. 69 (2015) 688–695.
[51] A. Lamacz, A. Rätz, B. Schweizer, A well-posed hysteresis model for flows in porous media and applications to fingering effects, Adv. Math. Sci. Appl. 21 (2011) 33–64.
[52] L.A. Richards, Capillary conduction of liquids through porous mediums, Physics 1 (1931) 318–333.
[53] H. Berninger, S. Loisel, O. Sander, The 2-Lagrange multiplier method applied to nonlinear transmission problems for the Richards equation in heterogeneous soil with cross points, SIAM J. Sci. Comput. 36 (2014) A2166–A2198.
[54] B. Schweizer, Regularization of outflow problems in unsaturated porous media with dry regions, J. Differential Equations 237 (2007) 278–306.
[55] A. Mikelić, A global existence result for the equations describing unsaturated flow in porous media with dynamic capillary pressure, J. Differential Equations 248 (2010) 1561–1577.
[56] X. Cao, I.S. Pop, Degenerate two-phase porous media flow model with dynamic capillarity, J. Differential Equations 260 (2016) 2418–2456.
[57] J.-P. Milišić, The unsaturated flow in porous media with dynamic capillary pressure, J. Differential Equations 264 (2018) 5629–5658.
[58] X. Cao, I.S. Pop, Uniqueness of weak solutions for a pseudo-parabolic equation modeling two phase flow in porous media, Appl. Math. Lett. 46 (2015) 25–30.
[59] F. Brezzi, M. Fortin, MIxed and Hybrid Finite Element Methods, Springer Series In Computational Mathematics, vol. 15, Springer New York, 1991.
[60] R. Eymard, C. Guichard, R. Herbin, R. Masson, Gradient schemes for two-phase flow in heterogeneous porous media and Richards equation, Z. Angew. Math. Mech. 94 (2013) 560–585.
[61] Q. Deng, An analysis for a nonoverlapping domain decomposition iterative procedure, SIAM J. Sci. Comput. 18 (1997) 1517–1525.
[62] A. Ern, I. Mozolevski, L. Schuh, Discontinuous Galerkin approximation of two-phase flows in heterogeneous porous media with discontinuous capillary pressures, Comput. Methods Appl. Mech. Engrg. 199 (2010) 1491–1501.
[63] G. Enchéry, R. Eymard, A. Michel, Numerical approximation of a two-phase flow problem in a porous medium with discontinuous capillary forces, SIAM J. Numer. Anal. 43 (2006) 2402–2422.
[64] K. Brenner, C. Cancès, D. Hilhorst, Finite volume approximation for an immiscible two-phase flow in porous media with discontinuous capillary pressure, Comput. Geosci. 17 (2013) 573–597.
[65] K. Bouadjila, A. Mokrane, S.A. Saad, M. Saad, Numerical analysis of a finite volume scheme for two incompressible phase flow with dynamic capillary pressure, Comput. Math. Appl. 75 (2018) 3614–3631.
[66] J. Droniou, R. Eymard, High-order mass-lumped schemes for nonlinear degenerate elliptic equations, SIAM J. Numer. Anal. 58 (2020) 153–188.
[67] G. Alzetta, et al., The deal.II library, version 9.0, J. Numer. Math. 26 (2018) 173–183.
[68] M.T. van Genuchten, A closed-form equation for predicting the hydraulic conductivity of unsaturated soils, Soil Sci. Soc. Am. J. 44 (1980) 892.
[69] M. Schneider, T. Köppl, R. Helmig, R. Steinle, R. Hilfer, Stable propagation of saturation overshoots for two-phase flow in porous media, Transp. Porous Media 121 (2017) 621–641.